Available online at www.sciencedirect.com

ScienceDirect

Coordination Chemistry Reviews 252 (2008) 32–56

COORDINATION CHEMISTRY REVIEWS

www.elsevier.com/locate/ccr

Review

Molecular switches for electron and energy transfer processes based on metal complexes

Joe Otsuki[a,**], Tetsuo Akasaka[b], Koji Araki[b,*]

[a] College of Science and Technology, Nihon University, Kanda Surugadai, Chiyoda, 101-8308 Tokyo, Japan
[b] Institute of Industrial Science, University of Tokyo, Komaba, Meguro, 153-8505 Tokyo, Japan

Received 15 January 2007; received in revised form 7 March 2007; accepted 7 March 2007
Available online 13 March 2007

Contents

Abstract

Molecular switches based on metal complexes, in which electron and/or energy transfer processes are switched on and off or significantly modulated by externally applied stimuli, such as electrons (redox reactions), light, and chemical substances (protons, ions, and molecules), are reviewed. Also described are single-molecule transistors, in which conductance through a single metal complex is modulated by applied gate voltages.

Keywords: Electron transfer; Energy transfer; Molecular devices; Molecular switches

1. Introduction

Manipulating electrons and photons at the molecular or supramolecular level may lay the foundation for potential applications in molecular photonic and electronic devices [1,2]. In putative molecular devices, individual molecules function as active components that play the role of wires, switches, diodes, transistors, and light-absorbing/emitting centers and so on. For the system to work in a cooperative fashion, communication between each component is critical. Electron and energy transfer processes [3–5] may serve as means of information transmission among molecules. Further, switching of the signal transmission is needed to perform logic operations. In this context, molecules that can switch electron and energy transfer processes will play the central role in molecular electronic/photonic devices.

Metal complexes have unique advantages in such applications [6], since the electronic states can be changed in a controlled fashion within easily accessible potential ranges. Spin states (high/low spin, spin quantum number) may be controlled by the strength and symmetry of the ligand field and redox states

---

* Corresponding author. Tel.: +81 3 5452 6363; fax: +81 3 5452 6364.
** Corresponding author. Fax: +81 3 3259 0817.
E-mail addresses: otsuki@chem.cst.nihon-u.ac.jp (J. Otsuki), araki@iis.u-tokyo.ac.jp (K. Araki).

0010-8545/$ – see front matter © 2007 Elsevier B.V. All rights reserved.
doi:10.1016/j.ccr.2007.03.005

of metal ions. Facilitated intersystem crossing from a singlet excited state to other multiplet states (e.g., triplet) for heavy metal atoms may be utilized to tune excited state energetics, lifetimes, emission spectra and efficiencies. Many of the transition metal complexes exhibit a sufficient excited state lifetime that permits various processes to occur, such as electron and energy transfer, which are essential to “wire” molecular components. Additional merit in the use of metal complexes is the ability to organize organic ligands in well-defined, predictable geometry.

In this review article, the development of molecular switches for electron and/or energy transfer processes based on metal complexes is overviewed. In these molecular switches, electron or energy transfer processes are switched on/off or largely modulated in response to externally applied stimuli. The switches are grouped into categories according to the kinds of external stimuli. Thus, redox-responsive systems and light-responsive systems are described in Sections 2 and 3, respectively. Chemical substance-responsive systems are treated in Section 4, which have relevance and implications for molecular sensors. In Section 5, a nascent field of single-molecule transistors is illustrated by recent prototypical devices based on metal complexes. Finally, in Section 6, the prospects of metal complex-based molecular switches are briefly discussed.

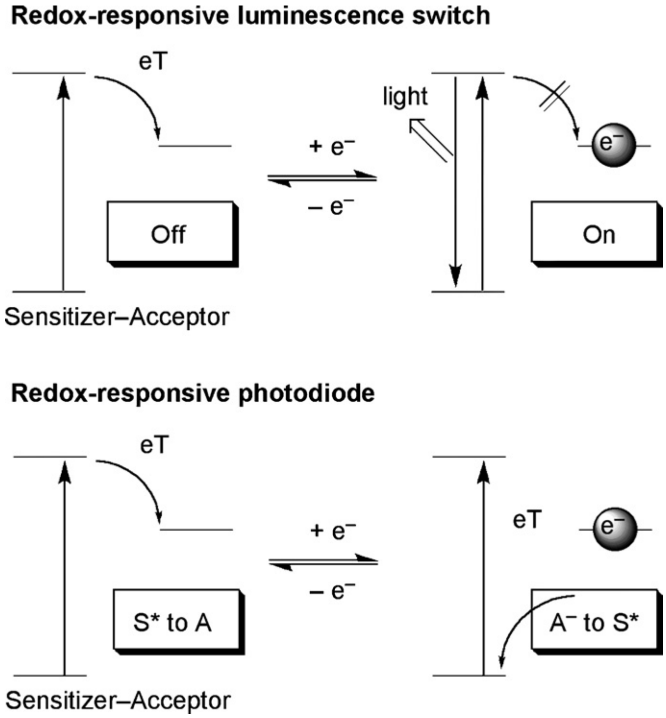

Fig. 1. Modes of operation for sensitizer–acceptor dyads as a redox-responsive luminescence switch and a photodiode. “Et” stands for electron transfer.

2. Redox-controlled switches

2.1. Redox-controlled electron transfer processes

Combining a light-emitting center (sensitizer) and a redox-active moiety (quencher) is a well-established motif in the redox-responsive luminescence switch. The redox active group must be reversibly interchanged between two redox states either chemically or electrochemically. The prerequisite for successful switching is that the luminescence from the emitting center is quenched by the redox-active group in one of the oxidation states but not in the other, as illustrated by the upper scheme in Fig. 1. In the oxidized form (left) of the luminescence switch comprising a sensitizer–acceptor pair, the excited state of the sensitizer is oxidatively quenched through electron transfer from the sensitizer to the acceptor. Upon reduction, this quenching path is nullified, since the acceptor already has an electron, resulting in the recovery of the luminescence of the pristine sensitizer.

The first implementation of this idea was realized by conjugate molecule **1** comprising a ruthenium tris(bpy) (bpy = 2,2′-bipyridine) complex covalently linked to a redox-active quinone/hydroquinone group [7] (Fig. 2) With the oxidized quinone, the excited state of the ruthenium center, that is, the triplet metal-to-ligand charge transfer (MLCT) state, is effectively quenched by electron transfer to the quinone group. On the other hand, luminescence is emitted from the ruthenium center in the reduced form, since hydroquinone does not act as a quencher.

Ruthenium complex **2**, which has an anthraquinone unit fused with one of the phenanthroline ligands through a phenazine moiety, works similarly by quinone/hydroquinone interconversion

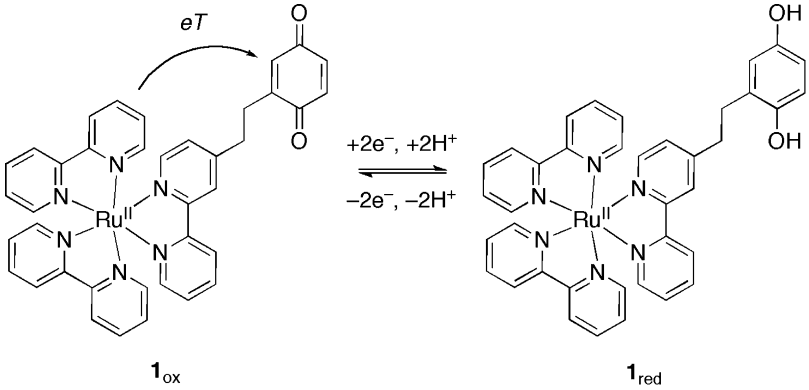

Fig. 2. Redox-responsive luminescence switch [7].

[8]. Metal complex **3**, in which a hydroquinone-functionalized 2,2′:6′,2″-terpyridine (tpy) ligand coordinates to a ruthenium(II) (4′-phenylethynyl-2,2′:6′,2″-terpyridine) fragment, also works as a redox-responsive luminescent switch [9]. In the hydroquinone form, the excitation of the MLCT absorption band produces an excited state, which leads to luminescence emission. Here it is noted that the phenylacetylenic group incorporated in one of the tpy ligands lowers the MLCT energy, preventing the promoted electron from thermally populating the metal-centered dd excited state. This mechanism renders the ruthenium tpy complex luminescent, which is otherwise non-luminescent at room temperature. Oxidation of the hydroquinone unit produces a quinone unit, which is an effective electron acceptor that traps the excited electron from the MLCT excited state, leading to an off state.

Fluorescence from the 1,4-disubstitued azine with ferrocene and pyrene units **4** is reversibly modulated by repeated redox reactions [10]. This compound is also made up of a fluorophore–quencher motif. In the neutral state, the fluorescence from the pyrene unit is quenched either by electron transfer from the ferrocenyl group to the excited pyrene unit or by energy transfer from the excited pyrene unit to the ferrocenyl unit due to a spectral overlap. In either case, the oxidation of the ferrocenyl unit renders the compound highly fluorescent, since the oxidized ferrocenyl unit has no ability to donate electron and the spectral overlap becomes small.

Redox-active transition metal macrocyclic complexes **5**–**10** are redox-responsive fluorescence switches. [11,12]. The sensitizer–quencher motif is realized in **5** by the combination of anthracene and a copper thiacyclam complex [13]. Both copper(I) and copper(II) states are accessible electrochemically. Copper(I) is a d^{10} metal ion and is inactive in interfering with the anthracene excited state, whereas copper(II) has a d^9 electronic configuration and thus can participate in an electron transfer process that accepts an electron from the anthracene excited state, quenching the fluorescence therefrom.

Nickel complexes **6** and **7** are fluorescence switches, in which the emission observed in the nickel(II) species is distinctly quenched on performing oxidation to the corresponding nickel(III) species [14]. The original fluorescence is restored upon reduction back to the nickel(II) species. For complex **8**, fluorescence from the naphthalene unit is observed in the state of nickel(II) [15]. A one-electron reduction to the corresponding nickel(I) species induces a distinct decrease in the emission intensity. Water-soluble **9** and **10** also work as redox-responsive fluorescence switches in a similar mode of operation as with the examples above [16].

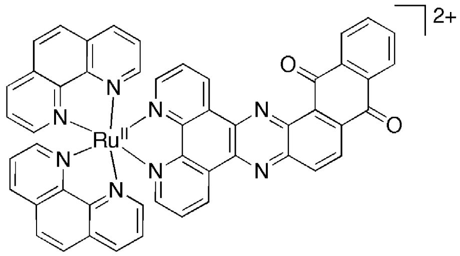

2

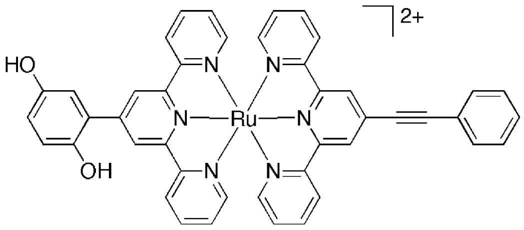

3

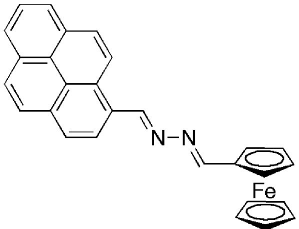

4

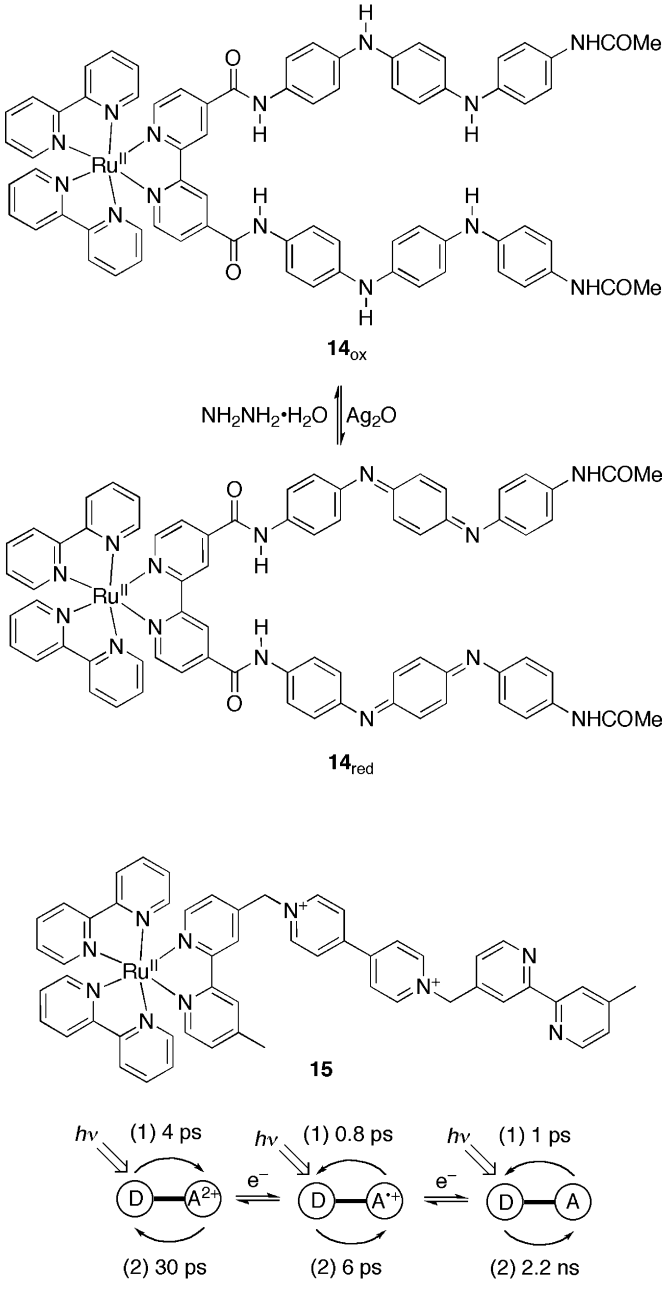

Fig. 3. Redox-responsive molecular diodes [19,29].

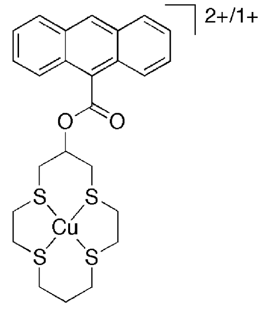

5

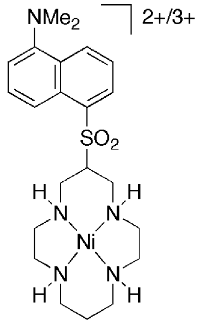

6

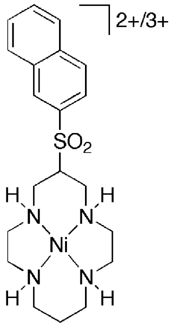

7

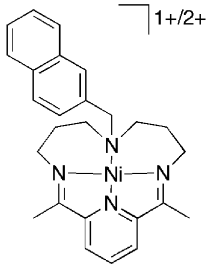

8

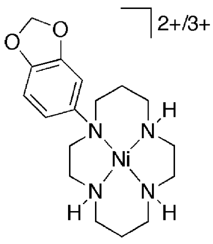

9

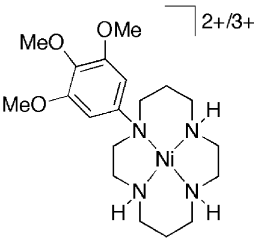

10

4,4″-Azobis(2,2′-bipyridine) has two chelating sites connected by a redox-active azo group. Mononuclear (**11**) and dinuclear ($\mathbf{12}_{\mathrm{RuRu}}$ and $\mathbf{12}_{\mathrm{OsOs}}$) ruthenium or osmium complexes have been prepared [17]. The excited state of these complexes is non-luminescent, which is characterized as a MLCT state wherein the promoted electron is located on the low-lying π^* orbital of the bridging azo ligand. One- and two-electron reductions occur on the bridging ligand. The reduced complexes, in which the additional electron is located on the bridging ligand, emit bright luminescence, since the promoted electron now goes to one of the terminal bpy ligands and thus the complexes behave more or less like the parent $[Ru(bpy)_3]^{2+}$ complex. Thus, these complexes can be considered to belong to the sensitizer–acceptor ($[Ru(bpy)_3]^{2+}$-azo) dyad system, but the acceptor unit is more integrated, structurally and electronically, to the sensitizer. Tetranuclear ruthenium complex $\mathbf{13}_{\mathrm{Ru4}}$ works as a redox-responsive luminescence switch based on the same mechanism as well [18].

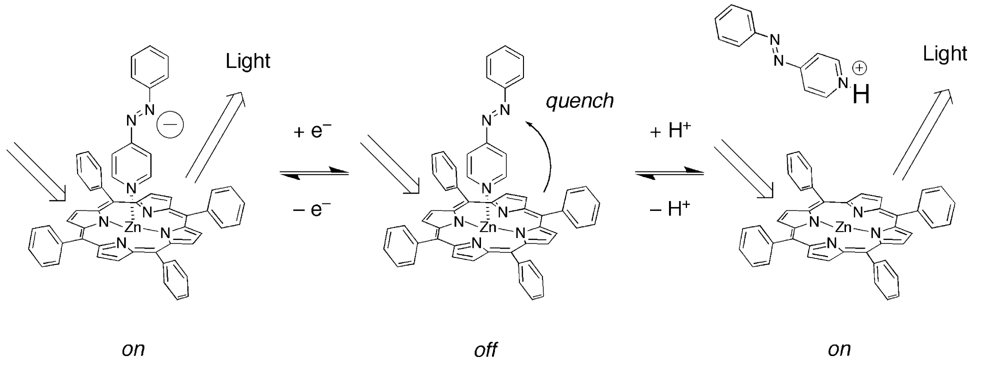

Fig. 4. Supramolecular redox- and proton-responsive photoswitch, **17**·ZnTPP. Adapted from Ref. [23].

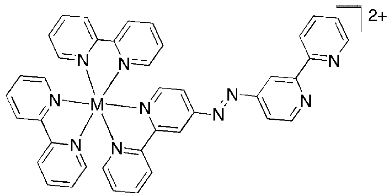

11$_{Ru}$: M = Ru
11$_{Os}$: M = Os

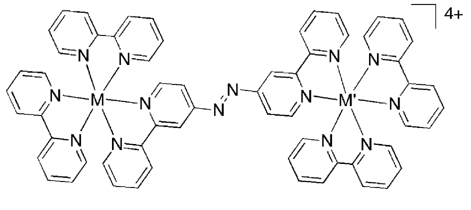

12$_{RuRu}$: M = M' = Ru
12$_{OsOs}$: M = M' = Os
12$_{RuOs}$: M = Ru, M' = Os

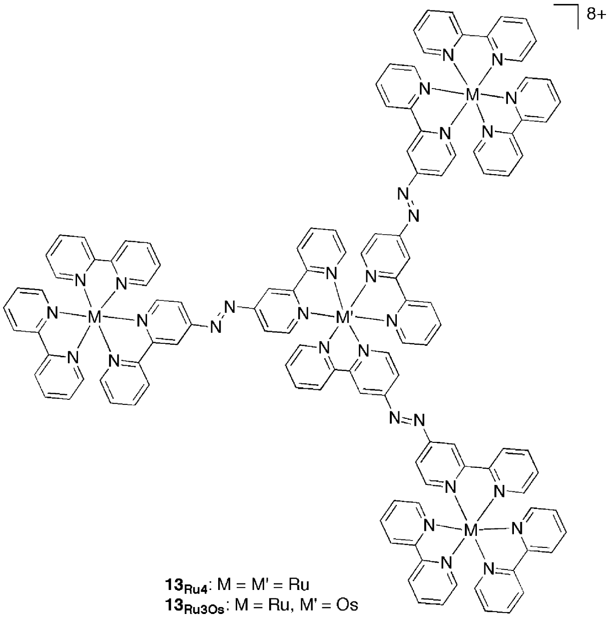

13$_{Ru4}$: M = M' = Ru
13$_{Ru3Os}$: M = Ru, M' = Os

In contrast to redox-responsive luminescence switches, redox-responsive photodiodes change the direction of electron transfer in response to redox input, as shown in the lower part of Fig. 1. The event taking place in the oxidized state is the same as the one in luminescence switches; the excited state is oxidatively quenched. Upon reduction, however, the sensitizer is still non-luminescent because of reductive quenching in the photodiodes. Thus, the direction of electron transfer is controlled by the oxidation state of the acceptor. A sensitizer–donor motif is also possible and a similar mechanism will work with the reversed direction of electron flow.

The ruthenium complex bearing *N*,*N*′-bis(4-aminophenyl)-1,4-phenylenediamine moieties **14**$_{red}$ can be considered as a molecular photodiode comprising a sensitizer–donor motif [19] (Fig. 3). It can be oxidized to give **14**$_{ox}$, which can again be reduced back to **14**$_{red}$. In both oxidation states, the complex is non-luminescent. It was proposed that donor-to-complex electron transfer is responsible for the quenching in **14**$_{red}$, while the reverse electron transfer from the complex to the oxidized donor is responsible for the quenching in **14**$_{ox}$.

4,4′-Bipyridinium (viologen) is a prototypical acceptor used especially in combination with ruthenium polypyridine complexes. Oxidative quenching of the luminescence of the ruthenium center in dyads in the form of ruthenium complex–viologen motif is well established. Reduction of the viologen fragment to the one-electron reduced monocation radical or to the two-electron reduced neutral species dose not enhance the fluorescence in the dyad **15** [20]. Instead, the reduced viologen works as an electron donor to reductively quench the ruthenium excited state. Detailed transient absorption study revealed the time constants for the electron transfer processes for each oxidation state. Fig. 3 summarizes the obtained forward as well as subsequent back electron transfer rates for each oxidation state of **15**.

A triad system represented by trimetallic complex **16** [21] is a step up in complexity from the dyads described above. In the initial state where the oxidation states of metals are represented by [Os^{II}–Ni^{II}–Pd^{II}], the excitation of the osmium center ([$^*Os^{II}$–Ni^{II}–Pd^{II}]) results in electron transfer to nickel to produce [Os^{III}–Ni^{I}–Pd^{II}] ($k_{eT} = 1.1 \times 10^8\ s^{-1}$, $\Phi_{eT} = 0.95$), since the nickel center is reduced in the least negative potential. It is then possible to reduce the nickel center electrochemically to prepare [Os^{II}–Ni^{I}–Pd^{II}] prior to photoexcitation. Excitation of the osmium center in this species leads to electron transfer to the palladium center on the other side of the molecule ($k_{eT} = 3.6 \times 10^7\ s^{-1}$, $\Phi_{eT} = 0.94$), since the nickel center is already in the reduced state. Thus, it is shown that the destination of a promoted electron by photoexcitation can be controlled by electrochemical input.

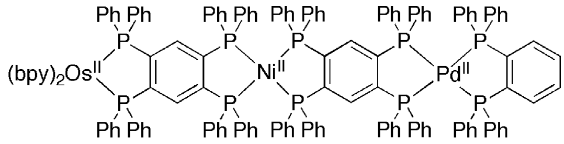

16

Zinc-porphyrin accepts one, and only one axial ligand perpendicular to the porphyrin macrocycle [22]. 4-Phenylazopyridine **17** is an excellent quencher of the fluorescence of zinc-porphyrin. It coordinates to the zinc ion in the porphyrin macrocycle through the nitrogen in the pyridine ring. In acceptor–sensitizer complex **17**·ZnTPP (ZnTPP = zinc-*meso*-tetraphenylporphyrin), the fluorescence is nearly completely quenched. Thermodynamic considerations suggest that the quenching is due to intracomplex electron transfer from the excited singlet state of the porphyrin to **17**. Indeed, electrochemical reduction of **17** deprives it of its acceptability and, as a consequence, the fluorescence of ZnTPP is restored, as illustrated in Fig. 4 [23]. Thus, complex **17**·ZnTPP functions as a redox-responsive fluorescence switch. The same supramolecule also functions as a proton-responsive fluorescence switch. This aspect will be described in Section 4.1.

Donor–sensitizer dyad **18**·ZnTPP is complementary to **17**·ZnTPP in the sense that the quenching is due to electron transfer from **18** to the excited singlet state of ZnTPP [24]. The selective oxidation of **18** leads to a partial recovery of the ZnTPP fluorescence. Re-reduction leads to quenching again.

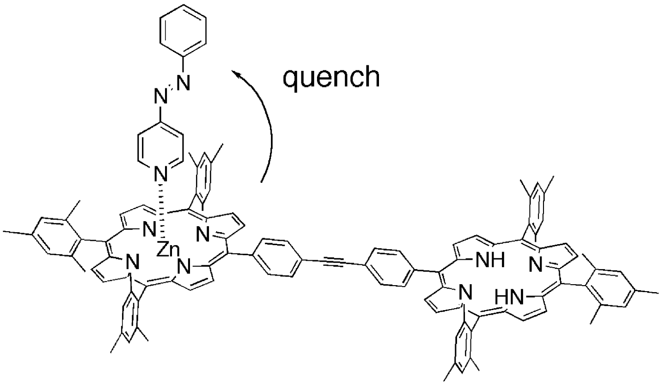

17·69

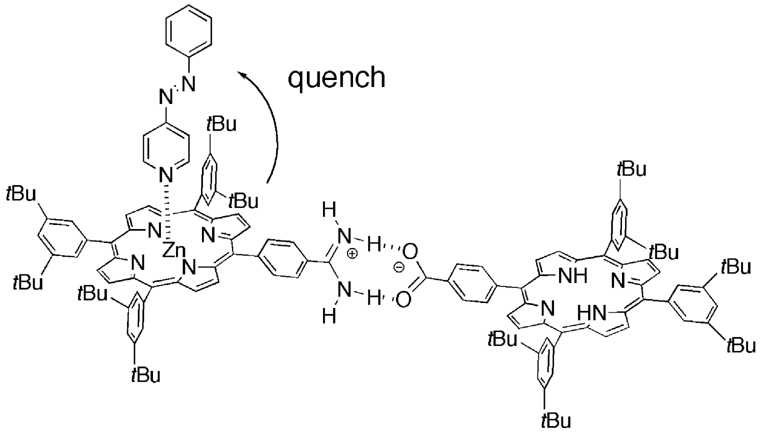

17·70·71

Sensitizer–acceptor dyad **19** was immobilized on nanocrystals of TiO_2, as shown in Fig. 5 [25–27]. The nanocrystal film is supported on a conductive glass electrode so that potentials can be applied to the TiO_2 nanocrystals. It was shown that the direction of photoinduced electron transfer is controlled to some extent by the applied potential to the electrode. A prototype of a write–read–erase device was fabricated based on this system [28]. The writing is done by photoirradiation to excite the ruthenium complex under a −0.45 V bias, which leads to the formation of a viologen radical cation. The viologen cation is colored due to a broad absorption around 600 nm. The color is erased by applying a positive voltage of 1.0 V to oxidize the viologen cation back to the original viologen dication.

Linear polynuclear metal string complexes embraced by polypyridylamide ligands are prospective molecular switching components. The dipyridylamido complex $\mathbf{20}_{red}$ contains three nickel(II) ions (Fig. 6). Crystallographic and magnetic studies showed that there is no formal metal–metal bonding in **20** [29].

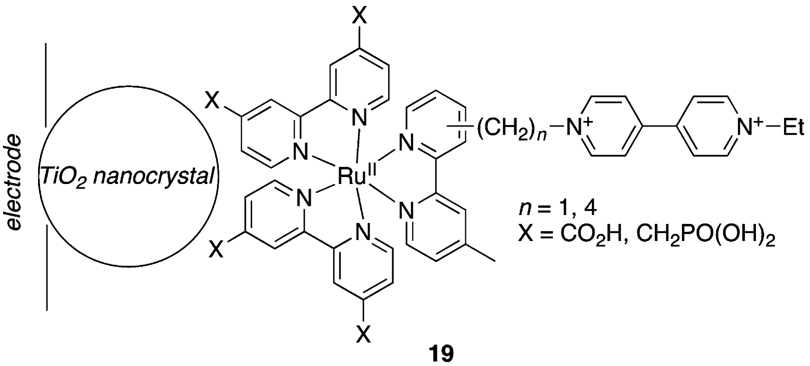

19

Fig. 5. Sensitizer–acceptor dyad immobilized on TiO_2 nanocrystals. Adapted from Ref. [25].

The reaction of $\mathbf{20}_{\mathrm{red}}$ with $AgPF_6$ results in one-electron oxidation concomittant with the removal of the terminal chloride ions to produce $\mathbf{20}_{\mathrm{ox}}$. The oxidation of $\mathbf{20}_{\mathrm{red}}$ to $\mathbf{20}_{\mathrm{ox}}$ makes the nickel–nickel separation shorter by 0.22 to 2.28 Å. The crystal structure and magnetic properties indicate the formation of delocalized nickel–nickel bonds [30]. A similar behavior was also found for longer pentanickel complexes **21** [31,32].

A family of string complexes **22** were subjected to scanning tunneling microscopy (STM) break junction measurements [33]. Among them, penta- and heptachromium strings exhibited two states corresponding to high and low conductivities. Under normal scanning measurements, stochastic on/off switching was observed. Although the mechanism behind the switching between the high and low conductivity states in these chromium string complexes remains to be addressed, it is possible that interchange between the localized and delocalized metal–metal bonding in these complexes is responsible for the switching.

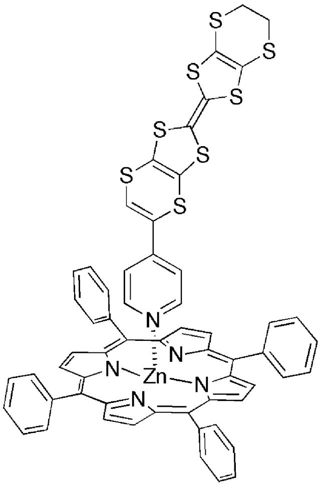

18·ZnTPP

2.2. Redox-controlled energy transfer processes

The previous section has seen various sensitizer–quencher dyads in redox-responsive luminescence switches. The fact that the luminescence is switched on/off implies that the excited-state lifetimes in the two states are significantly different. The on-state may have a long enough excited-state lifetime that can be followed by reactions via the excited state, such as energy transfer. Thus, by attaching a proper energy-accepting group to the sensitizer–quencher dyad, one can create redox-responsive energy transfer systems, such as the one shown in Fig. 7.

The multiporphyrin conjugates, linear gate **23** and T-gate **24**, shown in Fig. 8, are energy cascades, in which the excited energy levels decrease in the order of the boron–dipyrromethene dye, zinc-porphyrin, and free-base porphyrin [34–36]. Thus, the photoexcitation of the boron–dipyrromethene dye results, through a sequential excited energy transfer, in fluorescence output from free-base porphyrin. The excited state level of additional magnesium porphyrin lies close to zinc-porphyrin. One-electron oxidized magnesium porphyrin, however, has low-lying singlet excited states. This makes magnesium porphyrin an energy sink in its oxidized state. Thus, in the oxidized state, the fluorescence is switched off. The rate constants for the relevant processes are summarized in Fig. 8.

In the homonuclear ruthenium or osmium complexes containing 4,4″-azobis(2,2′-bipyridine), such as $\mathbf{12}_{\mathrm{RuRu}}$, the excited-state lifetime is significantly changed depending on the redox states of the azo ligand. In Section 2.1, these complexes are used as luminescence switches. The same mechanism can be used to make a redox-responsive energy transfer switch if an energy donor–acceptor pair is incorporated in the complex. Heterodinuclear ruthenium/osmium complex $\mathbf{12}_{\mathrm{RuOs}}$ is such a complex [37]. In this complex in the as-prepared state, both of the ruthenium and osmium complex units are non-luminescent, since the excited state is a low-lying MLCT state involving the bridging ligand. However, one- or two-electron reduction makes the complex behave like a typical ruthenium–osmium conjugate molecule, in which efficient energy transfer occurs from the excited ruthenium center to the ground-state osmium center. The final outcome is luminescence from the osmium center. Tetranuclear complex $\mathbf{13}_{\mathrm{Ru3Os}}$ contains an osmium complex unit in the center. The peripheral ruthenium complexes sensitize the osmium emission, a process gated by the redox state of the invervening bridging ligand.

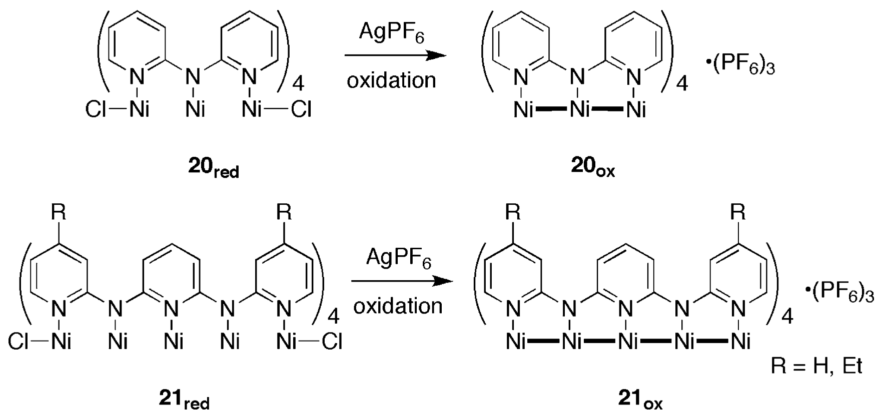

Fig. 6. Redox-responsive metal–metal bonds [30–32].

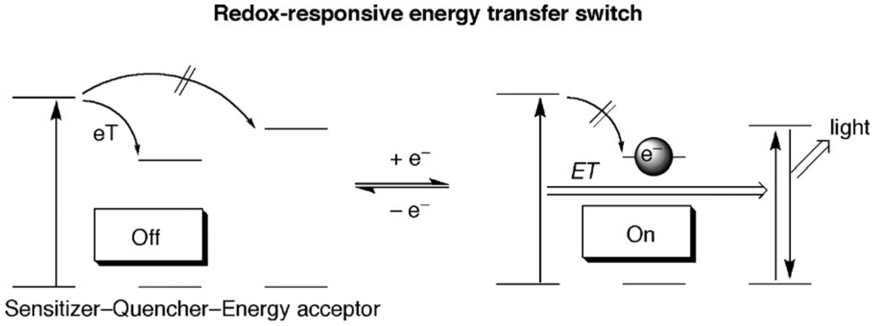

Fig. 7. Redox-responsive energy transfer switch. "ET" stands for energy transfer.

One problem associated with using bpy complexes [38] is that it is difficult to prepare geometrically well-defined multimetallic complexes. This is due to inevitable formation of isomers, such as optical isomers (Δ and Λ) and stereochemical isomers, when substituents are introduced on the bpy ligands (meridional and facial). One clever way to circumvent the problem is to use tpy units [39] instead of bpy. Introducing a substituent at the 4′-position (para to the nitrogen in the central pyridine ring) gives a stereochemically well-defined single compound. There are drawbacks, however, which are shorter excited-state lifetime and consequent non-luminescence properties of the ruthenium complex $[Ru(tpy)_2]^{2+}$, as compared to the bpy counterpart, $[Ru(bpy)_3]^{2+}$. In contrast, the osmium tpy complex $[Os(tpy)_2]^{2+}$ exhibits a better luminescence yield than the bpy counterpart, $[Os(bpy)_3]^{2+}$. The complexes bridged by the azobis(tpy) ligand (**25**) were prepared according to these considerations [40]. These complexes basically behave in a way similar to the bpy counterparts. Homonuclear ruthenium and osmium complexes are redox-responsive luminescent switches. Heteronuclear ruthenium/osmium complex $\mathbf{25}_{\mathrm{RuOs}}$ functions as a redox-responsive switch for intramolecular energy transfer. The on/off ratio of ≈30, which is defined by the ratio of luminescence intensity of the reduced species to that of the initial species, is greatly improved from that for $\mathbf{12}_{\mathrm{RuOs}}$ (≈2.5) because of two factors. One is that the non-luminescent nature of the ruthenium tpy unit makes the luminescence in the off-state very low. The other is the higher efficiency of the luminescence of the osmium tpy unit as compared to the osmium bpy unit in the on-state.

The geometrical advantage of the tpy complexes described earlier makes it possible to construct structurally well-defined linearly arranged multichromophore supermolecules, which are exemplified by triad chromophore compound **26** [41]. The triad is composed of coumarin, ruthenium(II), and osmium(II) units, where the latter two are connected via the same azoterpyridine bridging ligand as in **25**. In the triad, excited energy transfer occurs from one of the coumarin units to the ruthenium center. When the azo bridge is neutral, it functions as a quencher, but when it is reduced, a further energy transfer to the osmium terminal is realized. As coumarin 151 used in the triad has an absorption peak around 400 nm, the wavelength region where absorption by the ruthenium and osmium complex units is very small. Therefore, it is possible to selectively excite the coumarin moiety, resulting in an improved directionality of the energy transfer process.

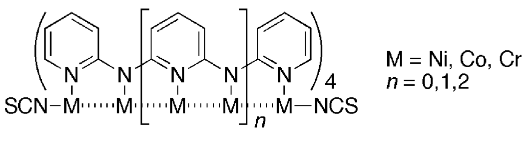

22

Preferred coordination numbers and geometry depend on the oxidation state of a metal ion. Thus, changing the oxidation state may alter the geometrical preferences of the metal, which, in a well-designed system, results in structural changes in the ligand sphere. Then, the structural change may have great impact on the electronic processes that we are interested in. The redox-responsive helicates shown in Fig. 9 is an example of a luminescence switch based on this mechanism [42]. Tetradendate ligand **27** or **28** wraps around a copper(II) ion to form a 1:1 complex, since the d^9 copper(II) ion prefers a tetragonal coordination. The copper(II) ion in this case can accommodate an additional ligand to form a five-coordinate species. Hence, in the presence of coumarin 343, the carboxylate group in the coumarin can coordinate to the copper(II) ion. The fluorescence of the coumarin fluorophore is quenched by the coordination due to the occurrence of an intramolecular process, which may be either electron or energy transfer in nature, involving the copper(II) center and the excited fluorophore.

The copper(II) ion can be reduced to a copper(I) ion, a d^{10} metal ion, which prefers a tetrahedral coordination environment. Upon reduction, the complex transforms into a 2:2 double helicate structure. In the course of this transformation, coumarin is released from the complex, since the copper ions are now coordinatively saturated in the double helix. As a consequence, the fluorescence of the pristine coumarin fluorophore is restored. Thus, this system functions as a redox-responsive fluorescence switch, in which the mechanism involves a large transformation of the structure of the complex, owing to the oxidation-state-dependent coordination preferences of a metal ion.

3. Light-controlled switches

Light has several advantages over other means as a control signal, which includes (i) fast processes (e.g., the excitation of molecules takes place in a timescale of femtoseconds), (ii) availability of advanced optics instruments (e.g., pulsed lasers, single photon counters, and "cheap" conventional detectors),

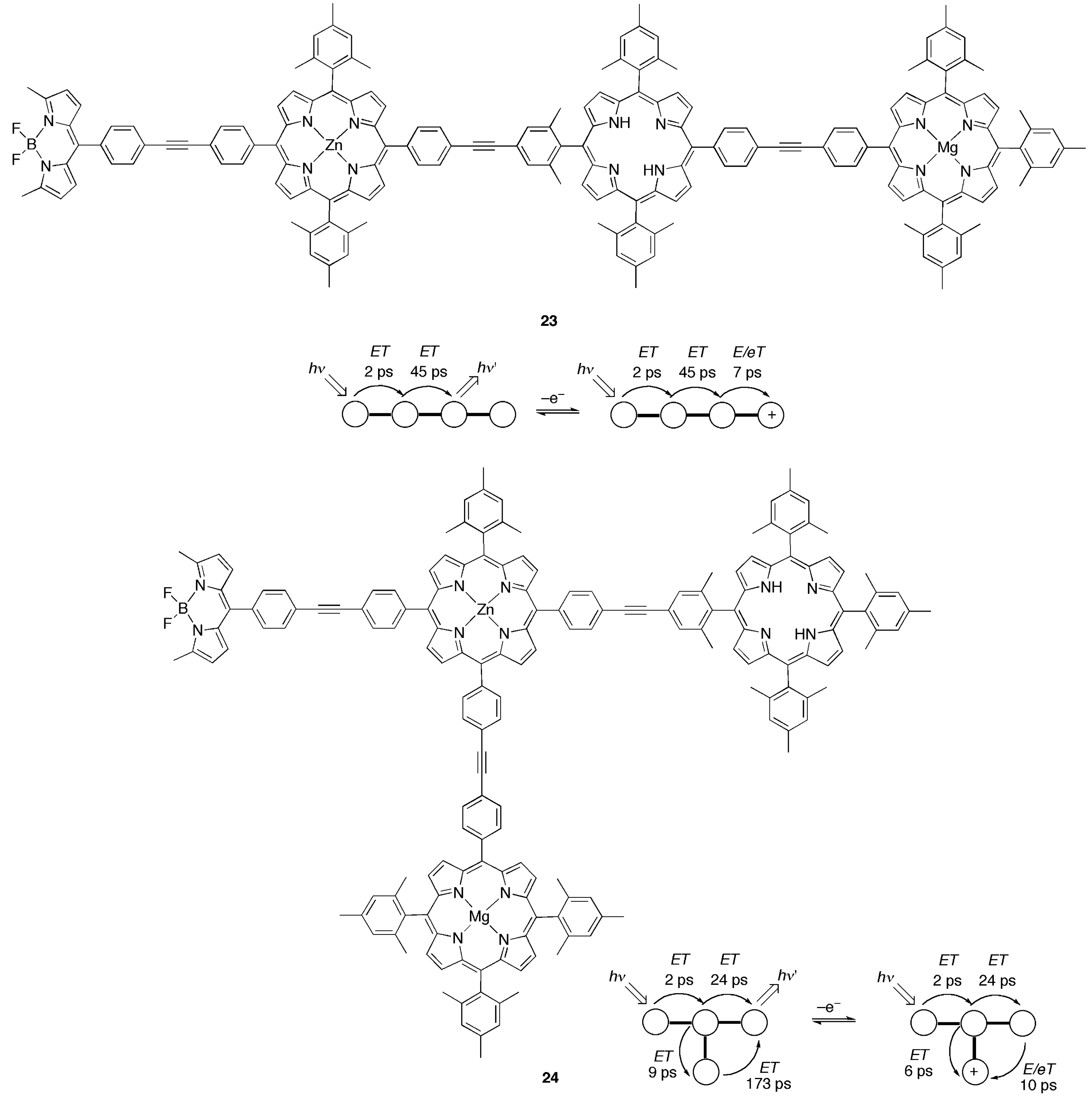

23

24

Fig. 8. Redox-responsive energy transfer switch based on porphyrin arrays [34–36].

(iii) parallel processability, and (iv) no materials involved (e.g., contamination free). However, one has to keep the drawbacks in mind as well. Especially, light cannot be focused into a single molecule. As a consequence, individual molecules in general are very "transparent". Simple arithmetic reveals that the probability (p) that a photon passing through an area (A in nm^2) containing a single molecule, whose molar absorption coefficient is ε in $M^{-1}\,cm^{-1}$, is given by: $p = 3.82 \times 10^{-7}\,\varepsilon A^{-1}$. As a typical case, say, in which light is focused in a spot with a diameter of 400 nm on a molecule with $\varepsilon = 10^4\,M^{-1}\,cm^{-1}$, the probability is only $p = \sim 3 \times 10^{-8}$. This concern is not a problem as long as experiments are carried out in bulk solutions. However, it will be crucial in downsizing light-controlled systems to a nanoscale.

Photochromic units are used as light-responsive gates in molecular systems. In the two forms that are interconverted by light, properties, such as absorption spectra, conjugation, and geometry, may be different, which in turn can be used as a switch for electron and/or energy transfer processes. Care must be taken in the use of photochromic units in combination with other electro/photoactive groups (e.g. energy/electron

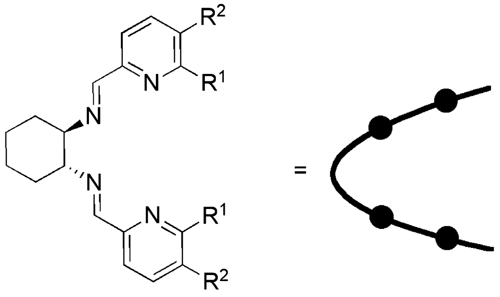

27: R^1^R^2 = benzo
28: R^1 = Me, R^2 = H

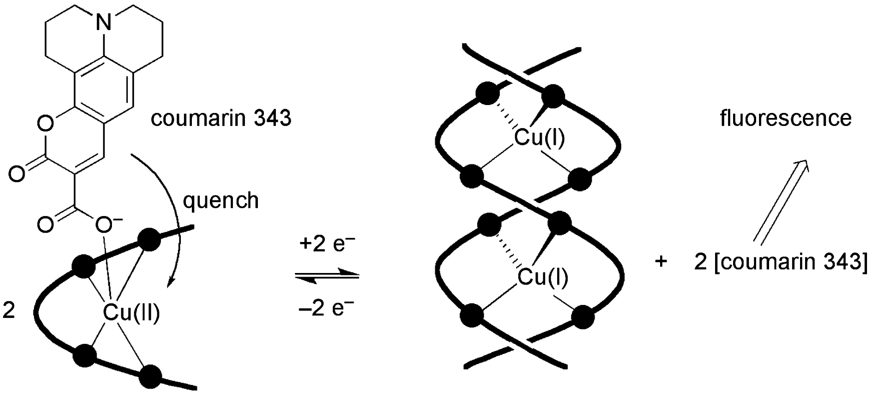

Fig. 9. Redox-responsive structural transformation and resulting fluorescence switching. Adapted from Ref. [42].

donors and acceptors), because these chromophores, when placed nearby, can interfere with photochromic activity. Indeed, we have learned from several reported examples (there are certainly many more not reported) that pristine photochromic properties can be drastically changed by the proximate electro/photoactive groups so that the desired properties, such as reversibility and thermal stability, are destroyed [43–45].

To realize electron transfer switches, the most straightforward system should be comprised of a donor–photochromic unit–acceptor motif. Upon light irradiation, the photochromic unit may change its conjugation and geometry to modulate interactions between the donor and the acceptor. A relatively small change in distance may have a large impact on the electron transfer rate, since the rate depends on the distance in an exponential fashion.

Sensitizer–photochromic unit–acceptor triad **29** is comprised of a sensitizer and a conjugate of photochromic unit and an acceptor [46]. Specifically, zinc-porphyrin, a stilbazole derivative, and pyromellitic diimide units are used as the respective components. Zinc-porphyrin and the other part of the supramolecule is connected through a labile, reversible axial coordination bond. An efficient electron transfer occurs when the bridge is in the *cis* form ($k_{\mathrm{eT}} = 1.83 \times 10^9\ \mathrm{s}^{-1}$, $\Phi_{\mathrm{eT}} = 0.77$) whereas no electron transfer is detected for the *trans* isomer. This is because of the distance change between the sensitizer and the acceptor associated with the photochromic *cis*/*trans* isomerization (Fig. 10).

An equilibrium shift in association/dissociation reactions by light irradiation can also be used to modulate electron transfer. The binding constants for the axial coordination of *cis*- and *trans*-3-phenylazopyridine derivatives, which have a bulky substituent on the 4-position of the pyridine ring, to zinc-porphyrins are significantly different. This is because of steric hindrance between the phenyl group of the ligand and the porphyrin macrocycle, which is effective only in the *cis* form, as shown with **30** in Fig. 11 [47,48]. Thus, photochromic interchange between the *trans* and *cis* forms causes a shift in the association equilibrium. Similarly, the degree of steric demand for 2-phenylazopyridine derivatives axially coordinated to zinc-porphyrin is different for the *trans* and *cis* isomers, but in a reverse sense. For 2-phenylazopyridine derivatives, the *trans* form experiences more steric repulsion than the *cis* form does, as illustrated by **31** in Fig. 11. Phenylazopyridines quench the fluorescence of zinc-porphyrin when axially bound. The most likely mechanism is electron transfer from excited porphyrin to phenylazopyridine. Thus, the photoinduced association/dissociation leads to the alteration of electron transfer, which can be read out through the fluorescence from zinc-porphyrin. The on/off ratios in terms of the fluorescence intensity so far achieved are not satisfactory, the best record being 2/1, which requires further improvement.

A series of linearly aligned multiple donor and acceptor units have been developed for use in femtosecond optical control of electron transfer processes. Tetrad **32** contains a pair of donor–acceptor pairs side-by-side in a D_1–A_1–D_2–A_2 motif [49]. A laser pulse to induce electron transfer in one of the donor–acceptor pairs followed by a second pulse to the other pair within the lifetime of the first charge-separated-state

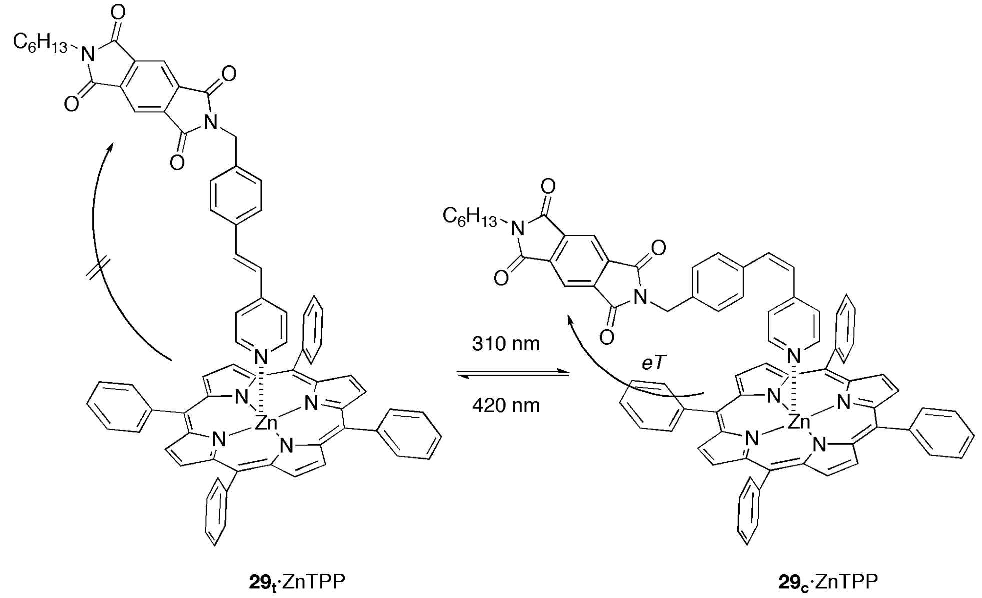

Fig. 10. Light-responsive electron transfer switch via modulation of sensitizer (donor)–acceptor distance. Adapted from Ref. [46].

leads to the formation of a long-range charge-separated- state, $D_1^+–A_1–D_2–A_2^-$.

Tetrad **33** also consists of a pair of donor–acceptor pairs but in a different sequence, $D_1–A_1–A_2–D_2$ [50]. This compound was used to examine the effect of a nearby dipole on electron transfer processes. In this compound, a 416 nm pulse produces $D_1^+–A_1^-–A_2–D_2$, while a 512 nm pulse produces $D_1–A_1–A_2^-–D_2^+$. These radical ion pairs have dipoles that affect electron transfer processes in the adjacent donor–acceptor pair. For example, the charge recombination reaction from the

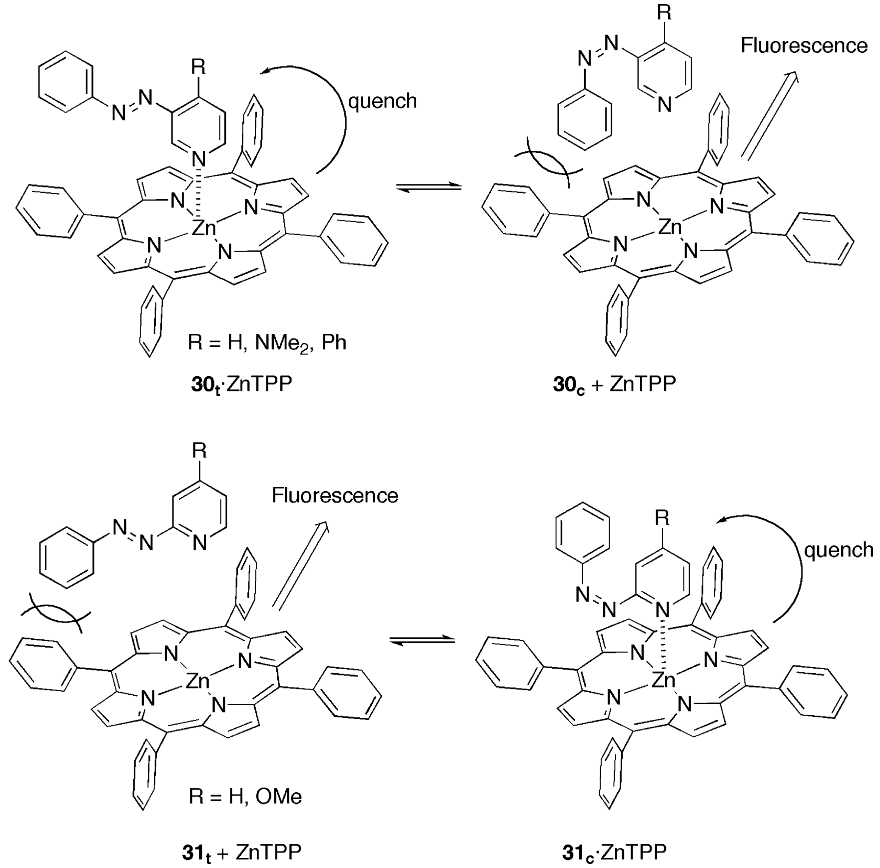

Fig. 11. Photo-controlled association/dissociation and modulation of consequent electronic processes. Adapted from Ref. [48].

state $D_1–A_1–A_2^-–D_2^+$ to the ground state occurs in 1.3 ns. In the presence of the nearby dipole, that is in the state $D_1^+–A_1^-–A_2^-–D_2^+$, the charge recombination in the $A_2^-–D_2^+$ pair occurs much more rapidly in 140 ps.

In tetrad **34**, which is another $D_1–A_1–A_2–D_2$ type molecule, a radical ion pair prevents a second charge separation from taking place [51]. For example, in the ground state compound, a 645 nm pulse irradiation is followed by electron transfer from D_1* to A_1 to form $D_1^+–A_1^-–A_2–D_2$. However, in the state, $D_1–A_1–A_2^-–D_2^+$, which can be produced by a 420 nm pulse, the electron transfer does not occur even with a 645 nm pulse irradiation.

Triad **35** demonstrates that the rate of electron transfer in a donor–bridge–acceptor array depends on the electronic state of the bridge [52]. The charge recombination reaction from $D^+–B–A^-$, which is produced by a 400 nm pulse irradiation, to the ground state occurs in a lifetime of 700 ns. When a second pulse at 520 nm is used to make the excited bridge, $D^+–B^*–A^-$, the charge recombination takes place in 100 ps. Thus, the electron transfer reaction through the excited bridge is accelerated 7000 times compared to that through the bridge in the ground state.

this compound is that the stability of the closed form toward the oxidation of the ruthenium center is low. It is reported that the oxidized closed form turns back to the open form in 5–10 min even without irradiation [53].

In **37**, ruthenium or osmium tris(bpy)-type complexes are connected through a dithienylethene unit [54,55]. In the open form, the metal-centered luminescence, which emanated from the MLCT state is observed. In particular, in the open form of the heteronuclear complex **37**(RuOs), an efficient energy transfer from the ruthenium center to the osmium center occurs [56]. The ^{3}MLCT emissions of these complexes are quenched upon conversion to their respective closed forms. This is due to energy transfer to the lowest excited states of the photochromic unit (Fig. 12).

Ethynylethene-bridged diferrocene **38** undergoes *E*/*Z* photoisomerization, as shown in Fig. 13 [57]. Cyclic voltammetry on the compound showed that the difference in the redox potentials for the oxidation of the two ferrocene units is 48 mV for the *Z*-form, while the difference is 70 mV for the *E*-form, which indicates that the electronic interactions are stronger in the *E*-form than in the *Z*-form.

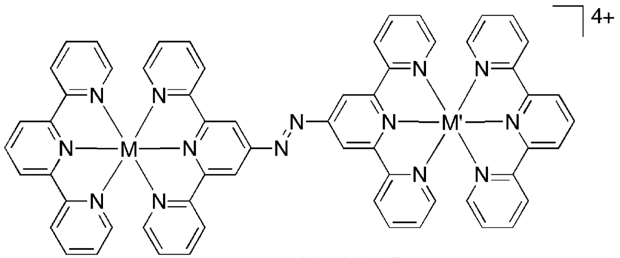

$\mathbf{25}_{\mathbf{RuRu}}$: M = M' = Ru
$\mathbf{25}_{\mathbf{OsOs}}$: M = M' = Os
$\mathbf{25}_{\mathbf{RuOs}}$: M = Ru, M' = Os

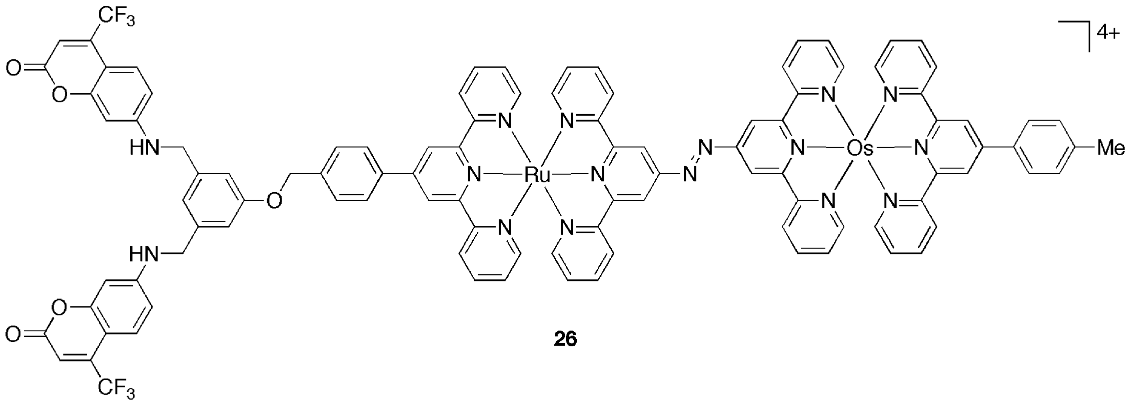

26

Cyclometalated ruthenium complexes are joined through a photochromic dithienylethene unit in **36** [53]. The dithienylethene in the open form undergoes a ring formation reaction to become a closed form under ultraviolet irradiation, which then turns back to the open form with visible light irradiation. An intervalence band is observed for the partly oxidized complex in the closed form, but not in the open form. Thus, the electronic communication between the two terminal complexes can be switched by light of different wavelengths. A problem in

In dinuclear complex **39**, two ruthenium complex units are appended onto a spiropyran photochrome, which undergoes interconversion between a spiro form and a dipolar merocyanine form [58]. Irradiation of ultraviolet light results in the formation of the merocyanine form. Molecular orbital calculations (ZINDO) show that the frontier orbitals (HOMO and LUMO) are extended over the linear bridging site in the spiro form, while they are rather localized on the merocyanine part in the merocyanine form. Thus, the electronic interactions can be represented

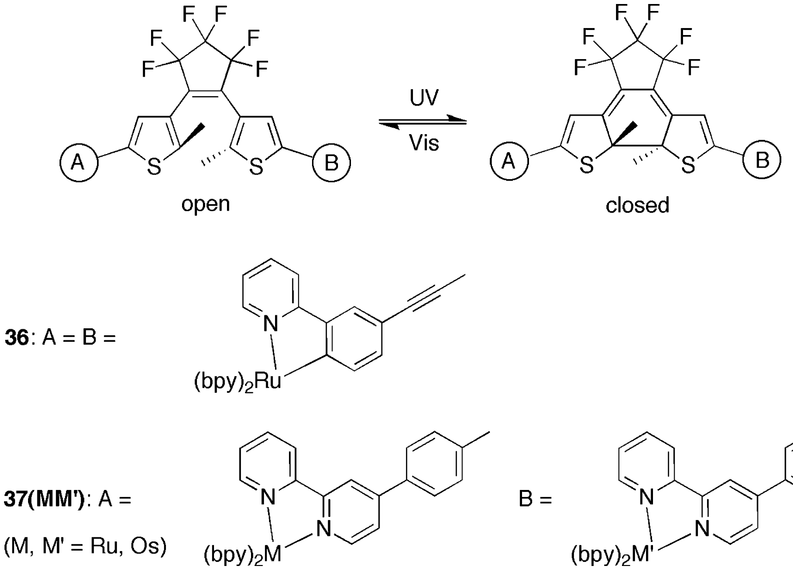

Fig. 12. Dithienylethene-bridged Ru/Os complexes [53–56].

as the circuit diagrams in the boxes in Fig. 14, for which the term “molecular T-junction relay” has been coined.

In **40a** and **41a** in Fig. 15, two anthracene fragments connected through a propylene chain are appended to a ruthenium tris(bpy) complex [59]. When the MLCT absorption band of this complex is irradiated, almost no luminescence emission is detected. This is due to the triplet energy transfer from the excited ruthenium complex to the anthracene unit. Irradiation into the singlet absorption band of anthracene at 390 nm causes the dimerization reaction to produce **40b** or **41b**. In **40b** and **41b**, excitation of the MLCT band of the ruthenium complex leads to a bright luminescence, because now there is no anthracene chromophore. Thus, the irradiation of the complex by 390 nm light turns the energy transfer off and luminescence on. The switching and memory performances have been demonstrated by polystyrene-immobilized complexes.

4. Chemical substance-controlled switches

Chemical species may be utilized as an external stimulus to modulate or switch electron/energy transfer processes, just like electrons and light. Proton is the simplest chemical species and, naturally, has been used most extensively. Other cations and anions, and even neutral molecules can be used as control signals via molecular recognition processes. This class of molecular systems is more often treated in the context of chemical sensors, since the outcome of the switching is often manifested by luminescence emission, which is useful for the analysis of the presence or concentration of the chemical species used as the control signal, which is actually an analyte in terms of sensor applications. Herein, we have summarized the present status of chemical substance-controlled processes according to the switching mechanisms of electron/energy transfer processes, rather than from the viewpoint of sensor applications in order to put these systems on an equal footing with other redox- and light-controlled switches.

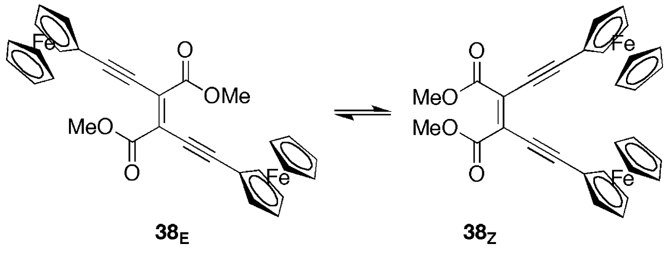

Fig. 13. Ethynylethene-bridged diferrocene, **38** [57].

4.1. Chemical substance-controlled electron transfer processes

There is a number of possible ways to control or switch on/off electron transfer processes by means of chemical species. Table 1 summarizes the modes of operation according to the chemical species as the control signal and the properties affected by the chemical species which are responsible for modulated electron transfer processes.

Protonation or cation complexation lowers the orbital energy and raises the oxidation potential of the complexed site. Deprotonation or cation decomplexation exerts exactly the opposite effect. By choosing an appropriate protonatable donor/acceptor

Table 1
Chemical substance-controlled electron transfer processes

Control signal	Affected properties	Examples
H^+	Redox potential of a donor	**42–45**
H^+	Intervening orbital energy	**46–49**
Anions	Intervening space	**50–52**
H^+	Position of a metal ion	**53**, **54**
H^+ (+redox)	Association/dissociation	**55·56·57** **55·58·59**
K^+/crown	Association/dissociation	**60·61**

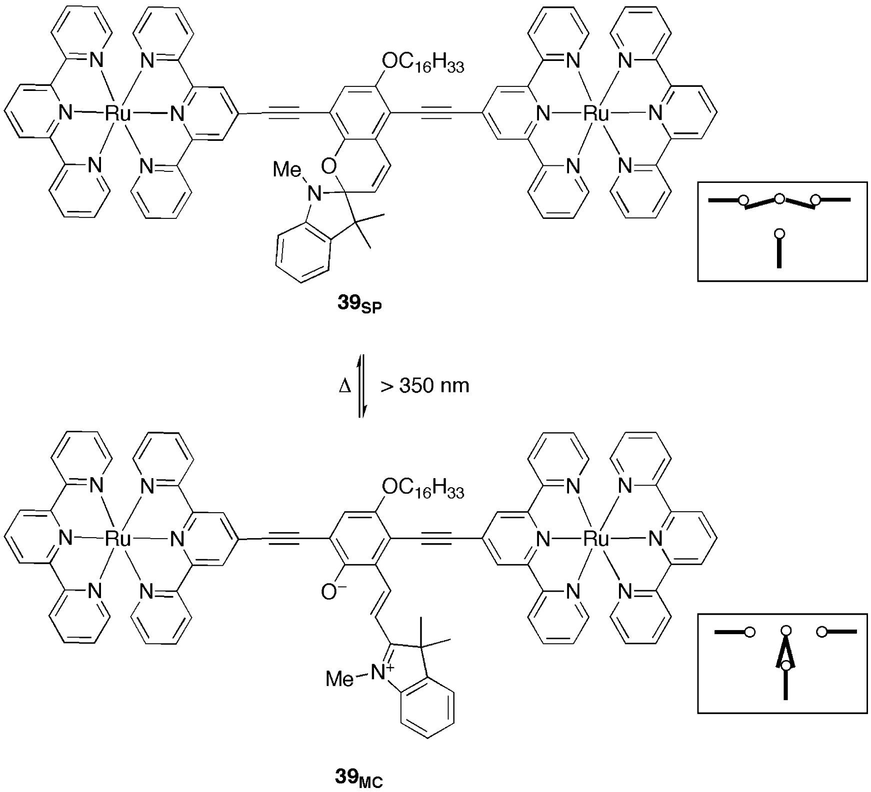

Fig. 14. Molecular T-junction relay [58].

pair, the electron transfer process can be switched on and off. Extensively developed photoinduced electron transfer (PET) sensors [60,61] are based on this mechanism. In PET sensors, a fluorophore (or luminophore) is connected to an electron transfer quencher, which doubles as a recognition site for the analyte. On binding the analyte, the redox potential is altered in a way that the electron transfer process is prohibited. The resulting intensified fluorescence is used as the output signal. The use of lanthanide complexes in this connection has distinct advantages. Lanthanide luminescence is characterized by long lifetimes up to milliseconds, long emission wavelengths, large stokes shifts, and line-like emission bands, which make it attractive particularly in applications for biological purposes [62,63]. Complexes **42** and **43** have tertiary amine groups as the electron donor to quench the excited tpy unit or the excited lanthanide ion [64]. Therefore, the complex is only weakly luminescent in neutral or alkaline solutions. Protonation of amine nitrogen raises the oxidation potential, so that electron transfer is not feasible any more. Thus, the delayed luminescence from the lanthanide ion is recovered with an enhancement factor of more than 10. Similarly, the luminescence of **44** is enhanced by over an order of magnitude when the azacrown units are bound by alkali metal cations, such as the potassium ion [65].

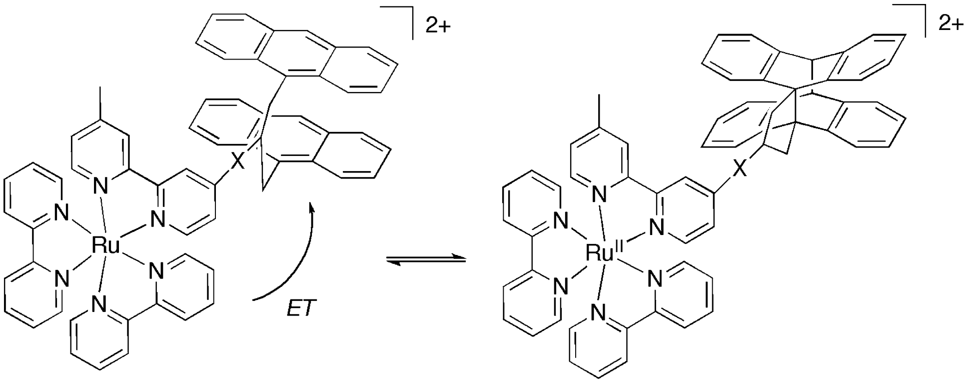

40a: X = CO_2
41a: X = CH_2O

40b, **41b**

Fig. 15. Light-responsive energy transfer switch [59].

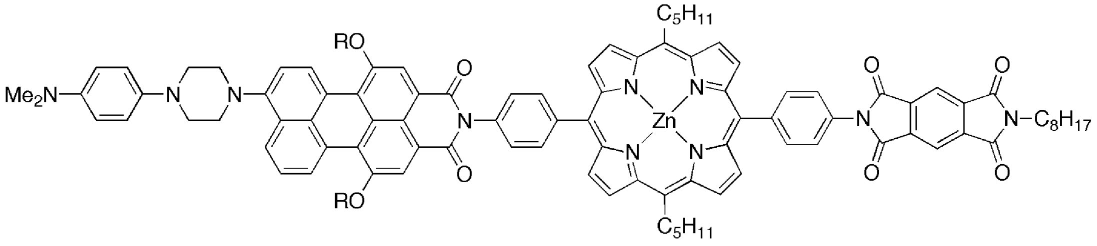

32: D_1–A_1–D_2–A_2

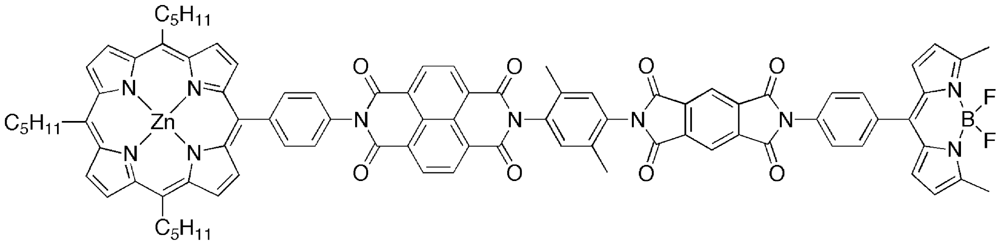

33: D_1–A_1–A_2–D_2

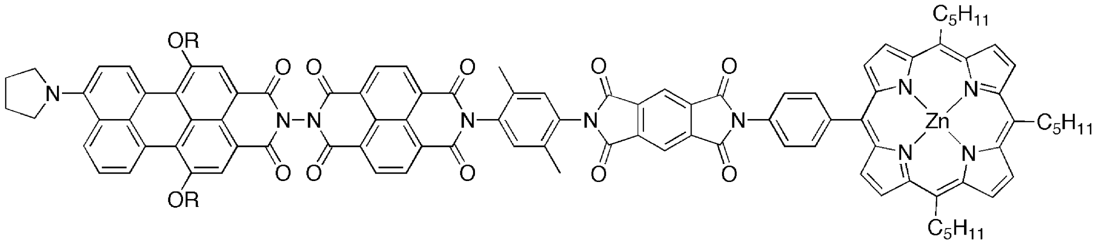

34: D_1–A_1–A_2–D_2

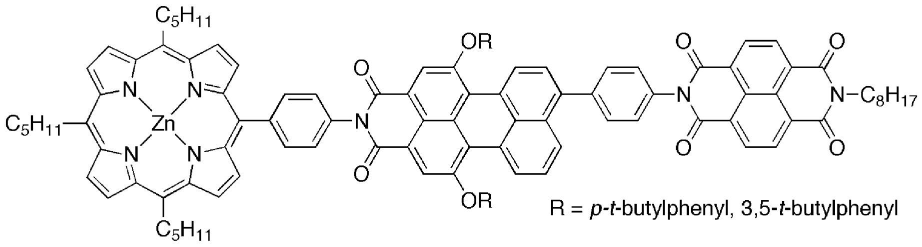

R = *p*-*t*-butylphenyl, 3,5-*t*-butylphenyl

35: D–B–A

Tetraazamacrocyclic nickel(II) complex **45** displays naphthalene fluorescence [66]. The diene macrocycle undergoes deprotonation (pK_a = 8.8) by a base to become the dienate shown in Fig. 16. The dienate species is distinctly less emissive than its dienic form, owing to a photoinduced electron transfer process that occurs only in the dienate form. Deprotonation lowers the oxidation potential for nickel(II) in the macrocycle by more than 0.6 V. Thus, reductive electron transfer is made possible only in the dienate form.

In metal–bridge–metal configurations, the bridge has a role as a conduit for mediating electronic interactions between the two metal centers located at both ends. The magnitude of the communication is measured by intervalence charge transfer absorption in the case of mixed-valence metal complexes [67–70]. If the bridge incorporates dissociable protons or protonation sites, the electronic interaction can be modulated by

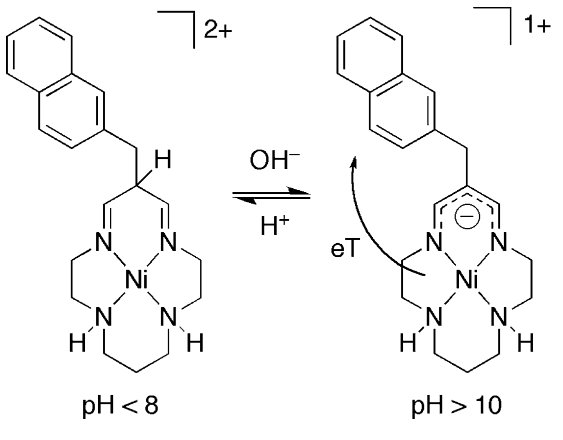

Fig. 16. pH-dependent diene/dienate conversion of **45** [66].

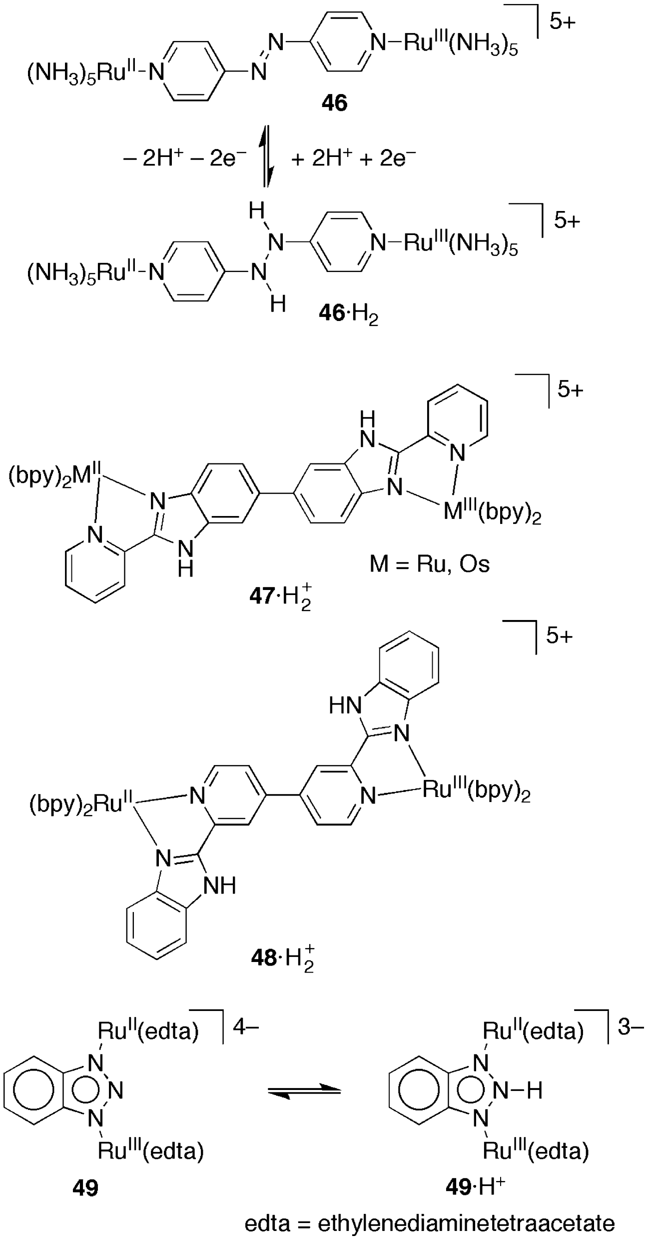

edta = ethylenediaminetetraacetate

Fig. 17. Proton-responsive electronic communication in mixed-valence complexes [71–74].

protonation/deprotonation on the bridge. Protonation (deprotonation) lowers (raises) the energy levels of frontier orbitals in the ligand, which in turn affects the ligand–metal orbital interactions, resulting in modulated through-bond interactions. Exemplary proton-responsive dinuclear metal complexes in this connection are shown in Fig. 17.

Dinuclear complex **46**, in which the pentaammineruthenium(II) group is bridged by 4,4′-azopyridine, undergoes interchange between the azo and hydrazine forms under different pH conditions [71]. Mixed-valence complexes of the type Ru^{II}–Ru^{III} can be prepared in both forms. Intervalence transition in the mixed-valence species indicates that the comproportionation constant, a measure of electronic interactions, is about $K_c = 40$ in the azo form. On the other hand, there is much weaker intervalence transition in the hydrazine form, indicating that the electronic interaction between the two ruthenium centers in the hydrazine form is much weaker than that in the azo form.

Dinuclear ruthenium complexes **47**·H_2^+ [72] and **48**·H_2^+ [73] are complementary with each other in terms of the orientation and connectivity of the (2-pyridyl)benzimidazole ligands in the bridge. In **47**·H_2^+, deprotonation enhances the electronic interactions between the metal centers. For the ruthenium complex, for instance, the coupling parameter values $H_{AB} = 60$–$80\,cm^{-1}$ for **47**·H_2^+ and 240–300 cm^{-1} for deprotonated **47** were obtained. On the other hand, for **48**·H_2^+ ($H_{AB} = 120\,cm^{-1}$) deprotonation decreases the metal–metal interaction, so that the intervalence transition is no longer observed.

In **49**, the electronic communication between the two ruthenium centers, as judged from the intervalence charge transfer absorption for the mixed valency state (Ru^{III}–Ru^{II}), is strong enough at pH > 3.3 that the complex belongs to the class III system, in which the electron is delocalized over the two metal centers [74]. Below pH 3, however, the interaction is diminished so that the complex now belongs to the class II mixed-valence system ($H_{AB} = 305\,cm^{-1}$), in which the electron is localized in one of the metal centers. The proton-switching effects were ascribed to geometric and electronic factors. The latter is owing to a better match in energy between the metal-based d_π orbitals and the deprotonated bridging ligand.

Ruthenium(II) and rhenium(I) bipyridyl complexes, **50** and **51**, respectively, bearing a calix[4]diquinone moiety connected via amide bonds, were prepared as anion sensors [75,76]. Due to an intramolecular oxidative quenching process by the quinone moieties, these complexes are only weakly luminescent. Binding of anions, such as chloride and acetate, in the macrocyclic cavity suppresses the electron transfer process, resulting in enhanced MLCT-based luminescence. In particular, acetate addition to **50** caused a luminescence intensity increase of up to 500%. One reason for the increased luminescence is that the anion binding decreases the interaction between the luminescent metal center and the quinone moieties. Another factor is that anion binding rigidifies the macrocycle and suppresses vibrational deactivation pathways, thereby elongating the excited-state lifetime.

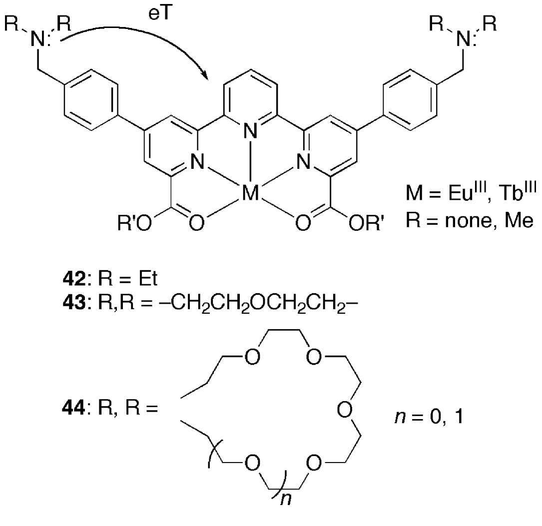

M = Eu^{III}, Tb^{III}
R = none, Me

42: R = Et
43: R,R = $-CH_2CH_2OCH_2CH_2-$
44: R, R =

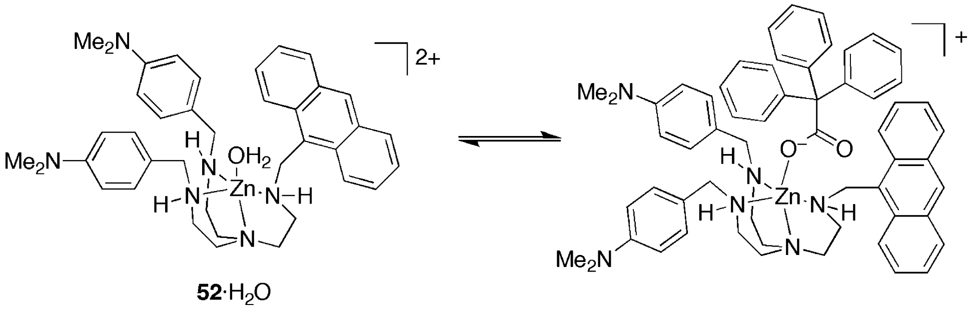

Fig. 18. Molecular curtain, which inhibits electron transfer when inserted between a donor and an acceptor [77].

In zinc complex **52** shown in Fig. 18, the zinc ion is surrounded around by a tripodal tetramine (tren) ligand, on which one anthracene substituent and two *N*,*N*′-dimethylaniline units are appended [77]. On excitation of the anthracene fragment, an intracomplex through-space photoinduced electron transfer process occurs. An electron moves from the dimethylaniline unit to the excited anthracene fragment. Thus, the anthracene fluorescence is weak. In the presence of one equivalent of triphenylacetic acid, the fluorescence becomes stronger as the electron transfer process is inhibited. It was proposed that the triphenylacetate coordinates to the zinc ion and fills the cavity, which interfaces the anthracene and dimethylaniline units, thereby preventing any occasional contact. The coordinated triphenylacetate behaves as an insulating "molecular curtain".

The pH-responsive translocation of metal ions is used to modulate electron/energy transfer processes in two-compartment ligands, **53** [78] and **54** [79], which are shown in Fig. 19. In each of the ligands, the compartment involving amide groups exhibits a lower affinity toward a metal ion than the other aromatic compartment. However, in basic solutions, the amide protons are dissociated to afford a stronger binding site for a metal ion. Thus, a metal ion is accommodated in the aromatic compartment below a certain pH value whereas the ion moves to the deprotonated amide compartment in more alkaline solutions. In **53**, nickel(II) is translocated from the aromatic compartment to the deprotonated compartment at pH > 9.5. In this species, in which the nickel ion is close to the anthracene fluorophore, electron transfer from the nickel ion to the singlet excited state of anthracene quenches the fluorescence. In **54**, the transition pH is around 9. At pH < 9, a copper(II) ion is in the aromatic compartment, while at pH > 9, the ion moves to the dianionic amide site. The trick in this switch is that the copper ion accepts an additional axial ligand only when it is chelated in the aromatic site. The fluorophore used in the system is coumarin 343, which coordinates to a metal ion only when its carboxylic group is deprotonated at pH > 5. The coumarin coordinates to the copper ion in the pH range of 5–9 in the end, of which fluorescence is quenched by the proximate copper ion through either an electron or energy transfer process.

In supramolecule **17**·ZnTPP, described in Section 2.1, the association of **17** and ZnTPP can be reversibly controlled by the addition of proton, since the coordination bond between **17** and ZnTPP is a labile bond. The added proton protonates the pyridine nitrogen, which becomes unable to coordinate to the zinc ion of porphyrin, leaving behind free ZnTPP. The freed ZnTPP emits bright fluorescence, as shown in Fig. 4. The addition of a base reverses the course of the reaction and the fluorescence is quenched again.

Pseudorotaxanes **55**·**56**·**57** [80] and **55**·**58**·**59** [81] are considered as molecular-scale analogs of electrical components, which are joined through "extension cables" that can be connected by "plugs and sockets". The crown ether moieties are considered as sockets, while the quaternary ammonium unit and the bipyridinium unit play the role of plugs. The two different types of socket-and-plug sets are connected/disconnected independently by different external inputs. The ammonium/crown ether complex is assembled/disassembled by an acid or a base, while the binding of the bipyridinium/naphthalene polyether complex is controlled by redox reaction. In ternary assembly **55**·**56**·**57**, photoexcitation of the ruthenium complex is followed by electron transfer to the bipyridinium acceptor ($k_{\mathrm{eT}} = 2.8 \times 10^8\ \mathrm{s}^{-1}$). On addition of a base, the luminescence intensity is enhanced, as the base extracts the ammonium proton to disconnect the plug from the socket. In **55**·**58**·**59**, the photoexcitation of the ruthenium complex is followed by an electron transfer process to the distal bipyridinium unit, which is indirectly joined by extension cable **58**. The rate constant for the electron transfer process within the triad is $k_{\mathrm{eT}} = 1.0 \times 10^7$ or $1.4 \times 10^8\ \mathrm{s}^{-1}$, likely depending on the conformations.

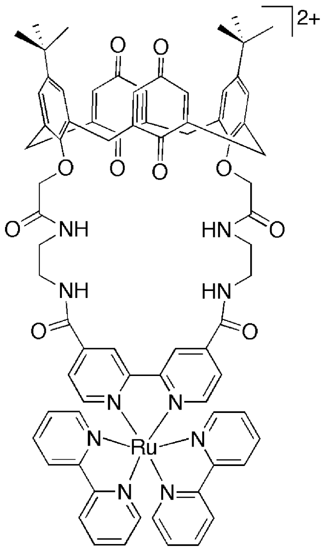

50

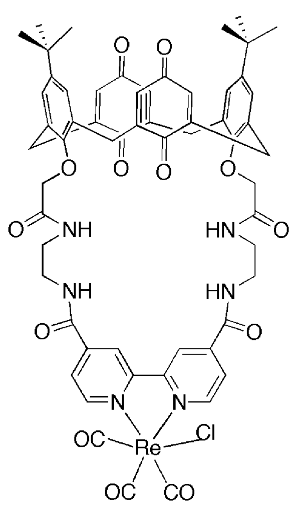

51

Association/dissociation of a sensitizer/acceptor pair in supramolecule **60·61** is realized by the alternate addition of a potassium ion and 18-crown-6 ether [82]. Zinc-porphyrin **60** is appended with a crown ether moiety. The fullerene derivative, appended with a cationic ammonium group, is an electron acceptor. On mixing, the two form a complex by the affinity of the ammonium ion with the crown ether moiety. In this state, photoinduced electron transfer occurs from the excited singlet state of zinc porphyrin to the fullerene moiety. The addition of the potassium ion dissociates the complex, resulting in an enhanced porphyrin emission. This is because the added potassium cation replaces the ammonium cation from the crown ether cavity. Further addition of 18-crown-6 ether extracts the potassium cation from the crown moiety in **60**, resulting in the reformation of the supramolecular complex.

Table 2
Chemical substance-controlled energy transfer processes

Control signal	Affected properties	Examples
H^+	Excited energy dissipation	**62**, **63**
H^+	Energy level	**64–66**
H^+	D–A distance	**67**, **68**
DMAP/H^+	Excited energy dissipation	**17·69·17·70·71**
Cu^{2+}/EDTA	Excited energy dissipation	**72**
Anions	Association/dissociation	**73**·coumarin

4.2. Chemical substance-controlled energy transfer processes

There is a number of possible ways to control or switch on/off energy transfer processes by means of chemical species, as summarized in Table 2.

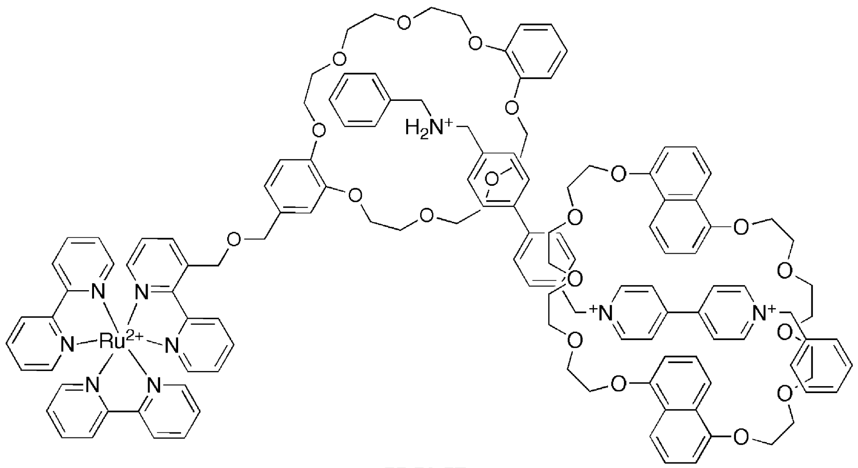

55·56·57

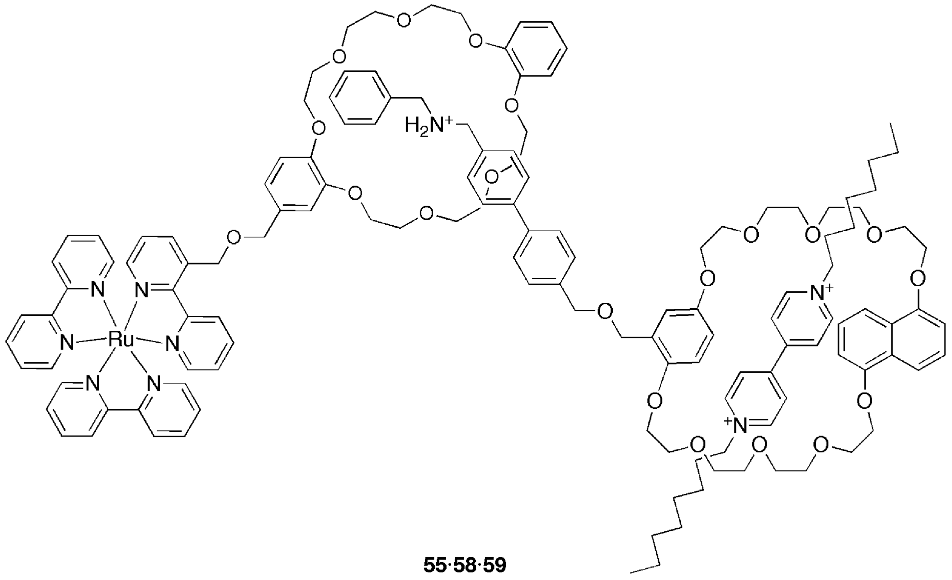

55·58·59

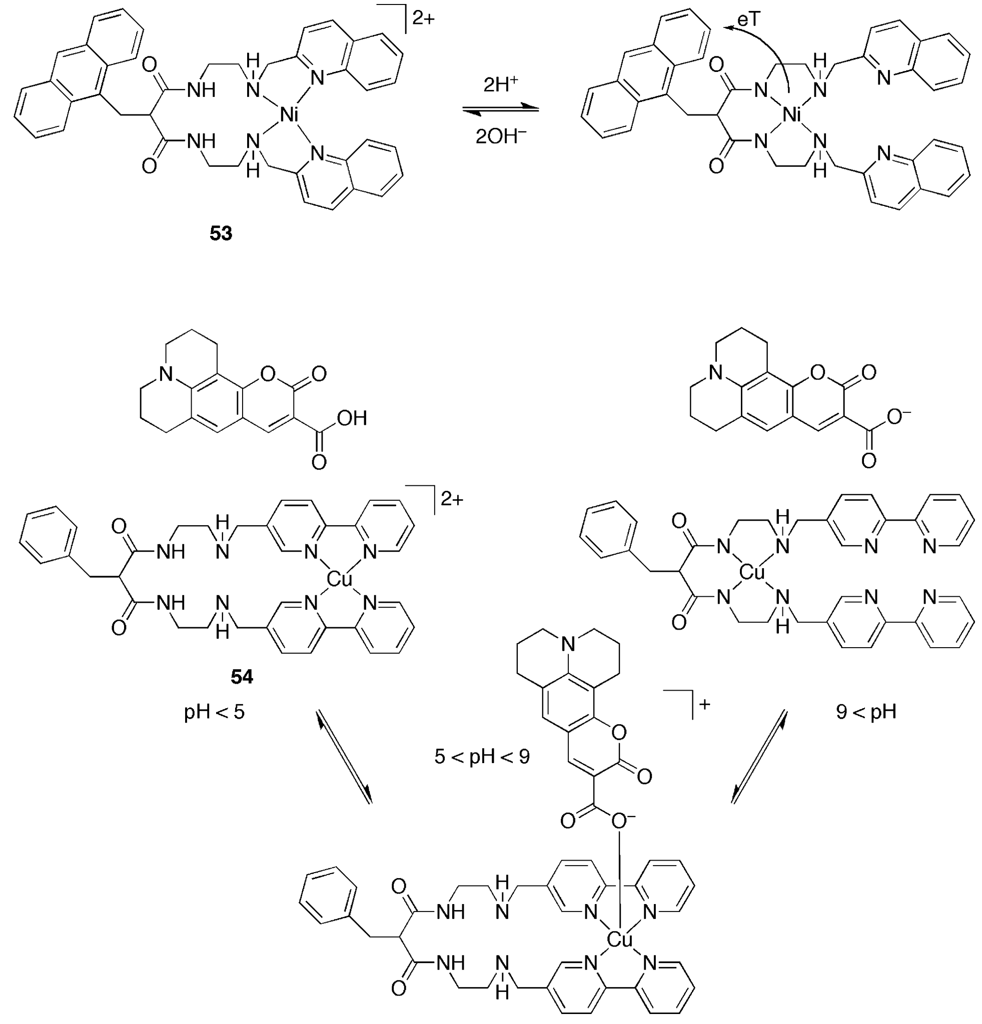
53

54

Fig. 19. pH-controlled translocation of metal ions [78,79].

Ruthenium tris(bpy)-type complexes containing 7-amino-dipyrido[3,2-a:2′,3′-c]phenazine [83] as one of the ligands are useful photosensitizing units. Efficient energy transfer is observed to an acceptor group connected to the amino terminal of dipyridophenazine via an amide bond [84]. This unit was employed to construct dinuclear ruthenium/osmium complexes **62** and **63** [85]. Energy transfer occurs from the excited ruthenium unit to the osmium unit in these complexes. It was demonstrated that energy transfer is switched off/on reversibly by protonation/deprotonation of the dipyridophenazine moiety. Protonation of phenazine nitrogens facilitates non-radiative deactivation of the MLCT state of the ruthenium center. The use of 4,4′-diphenyl-2,2′-bipyridine for the terminal ligands in **63** is advantageous because a complex containing this ligand exhibits larger light absorptivity and a longer excited-state lifetime than a complex with pristine bpy ligands. Indeed, the energy transfer efficiency in the on-state in **63** (0.98) is even more improved than the already high value of 0.90 in **62**.

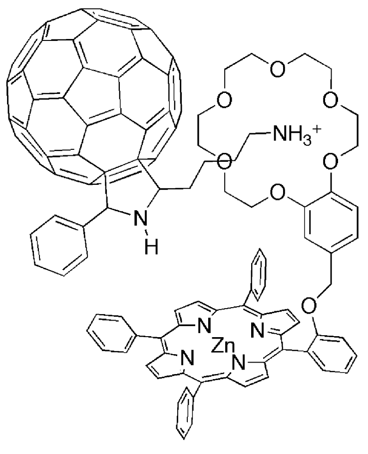
60·61

Since the formation of lanthanide excited states must be sensitized by energy transfer via the triplet state of an organic ligand [62,63], the efficiency of the intersystem crossing in the formation of the triplet excited state of the ligand and the energy level of the thus formed triplet state are crucial in efficient sensitization. In **64**, in which a dancyl fluorophore is appended to a europium complex unit, an effective sensitization does not occur due to inefficient intersystem crossing in the dancyl unit [86]. However, upon protonation of the dimethylamino group in the dancyl unit (pH < 4), an efficient energy transfer process takes place, since the intersystem crossing becomes efficient and the triplet energy ($E_T = 20{,}620\,\text{cm}^{-1}$) lies somewhat higher than the europium emissive state ($^5D_0 = 17{,}240\,\text{cm}^{-1}$). In the terbium complexes, **65** [87] and **66** [87,88], in which a phenanthridine moiety is appended, protonation to the phenanthridine nitrogen (pH < 6) lowers the triplet state energy of this unit from 22,000 to $21{,}300\,\text{cm}^{-1}$. The latter is higher than the terbium emissive state ($^5D_4$, $20{,}500\,\text{cm}^{-1}$) by only $800\,\text{cm}^{-1}$. Therefore, deactivation of the terbium complex by a back energy transfer process becomes much more efficient for the protonated form. The green luminescence is then switched off.

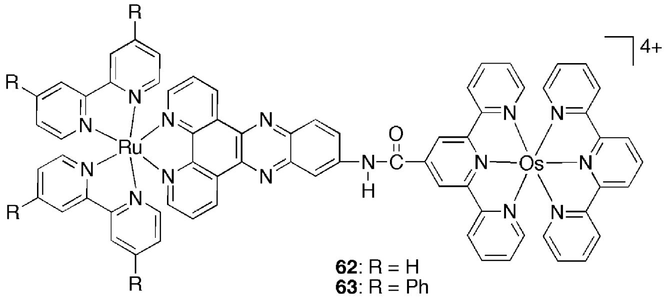

62: R = H
63: R = Ph

The nickel(II) complex of the cyclam tethered to a side chain, **67**, is named "scorpionand," because the tail stings the chelated metal center from the top (Fig. 20) [89]. In pH < 3, the amine group in the side chain is protonated and is forced away from the macrocyclic ring due to electrostatic repulsive effects. On raising the pH value above 3, the ammonium proton is released and the amine coordinates to the nickel ion, affording a six-coordinated species with an additional water coordination, **67**·H_2O. In this complex, the anthracene fragment is placed close to the nickel ion. As a result, the anthracene fluorescence is quenched to 60% of the intensity that is observed below pH 3. The quenching is ascribed to an energy transfer process on the basis of low temperature experiments. Upon further raising the pH value above 9, the bound water molecule dissociates to become a hydroxide ion (**67**·OH^-). The oxidation potential of the nickel(II) ion is thus lowered, so that an electron transfer process occurs from nickel(II) to the excited anthracene unit. This confers an additional quenching pathway and the anthracene fluorescence is nearly completely quenched. Thus, complex **67** is a three-valued fluorescence switch: high (pH < 3)/low (3 < pH < 9)/off (9 < pH).

Nickel(II) complex **68** is another scorpionand [90]. A dancyl group is the fluorophore, which is far apart from the metal ion in acidic solutions (pH < 4). On raising the pH values, the sulfonamide group deprotonates and coordinates to the nickel center. As a result, the fluorescence of the dancyl group is quenched. Dexter-type energy transfer has been inferred as the mechanism behind the fluorescence quenching. On further raising the pH values (pH > 7), a coordinated water molecule deprotonates, affecting the energy transfer efficiency and as a result the fluorescence is partially restored. Thus, this complex functions as another three-valued switch: high (pH < 4)/low (4 < pH < 7)/middle (7 < pH).

The system shown in Fig. 4 has been extended into a switch for intramolecular energy transfer. The ZnTPP is replaced by a dyad consisting of zinc-porphyrin and free-base por-

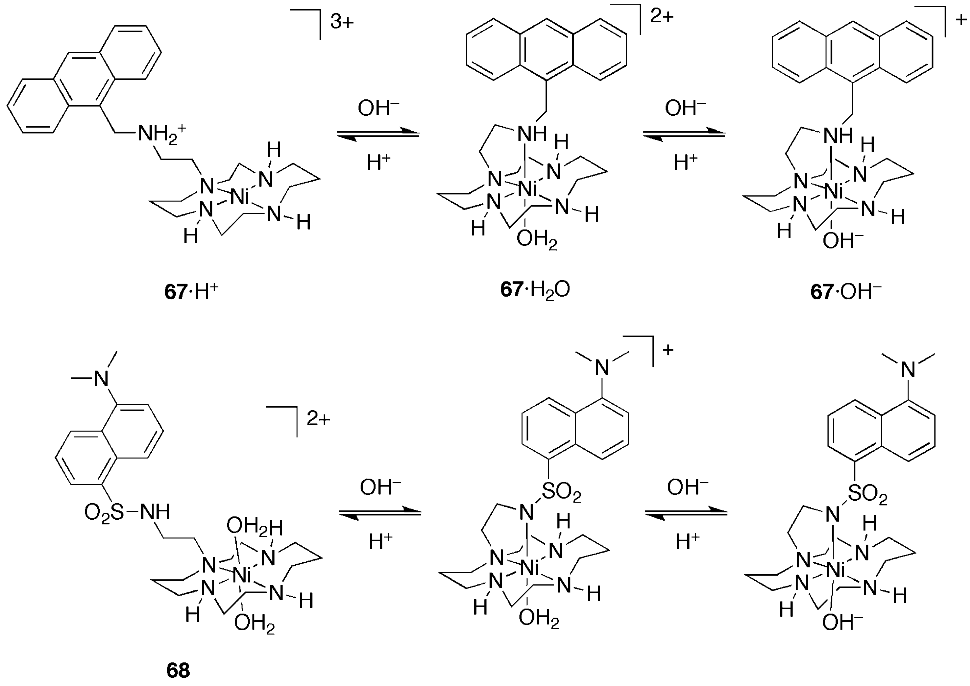

Fig. 20. Proton-responsive scorpionands [89,90].

phyrin, **69**. In **69**, a very efficient energy transfer occurs from the excited zinc-porphyrin to the free-base porphyrin unit ($k_{ET} = 4.2 \times 10^{10}\ s^{-1}$, $\Phi_{eT} = 0.99$), from which fluorescence is emitted [36,91–93]. The addition of **17** to a solution of **69** results in the formation of the complex **17**·**69** [94]. In this complex, energy transfer is switched off, as can be seen from the disappearance of the sensitized fluorescence from the free-base porphyrin unit. This means that the quenching of the excited state of the zinc-porphyrin unit by **17** is very rapid. To turn the switch on, the addition of *N*,*N*-dimethyl-4-aminopyridine (DMAP) is effective. Since DMAP is a stronger base than **17**, it replaces **17** from the coordination site. Furthermore, since it is not an electron acceptor, the energy transfer process is recovered. The addition of an appropriate amount of acid turns the switch off again. This is because the added proton selectively protonates and dissociates DMAP from the porphyrin, to which **17** can now coordinate.

As already demonstrated by several examples described in this and previous sections, non-covalent construction is a powerful methodology to create functional, elaborate molecular systems. To further develop the strategy, a ternary non-covalent complex consisting of a sensitizer, an acceptor, and a quencher, **17**·**70**·**71**, has been constructed in a modular manner [95]. The sensitizer and the acceptor are joined through an amidinium–carboxylate salt bridge. The excited energy transfer in the supramolecular dyad takes place very rapidly, at a rate ($k_{ET} = 4.0 \times 10^{9}\ s^{-1}$, $\Phi_{ET} = 0.89$) one order of magnitude larger than the Förster mechanism predicts [96]. The energy transfer is turned off with the coordination of **17–70**. Then the switch is turned on again by the addition of DMAP.

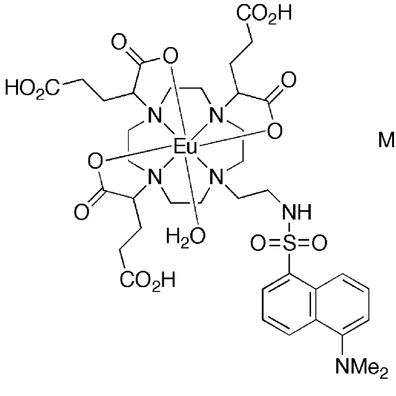

64

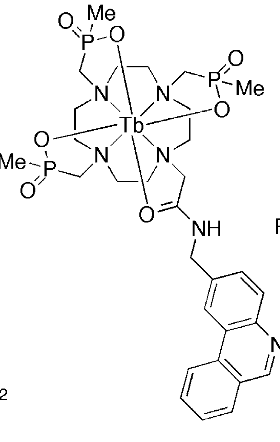

65

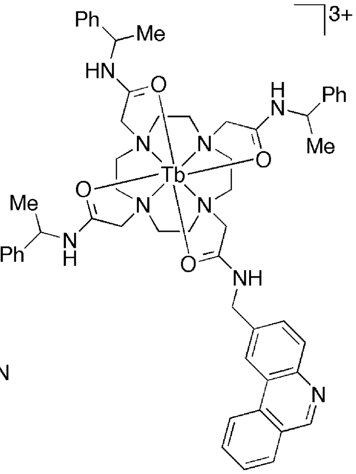

66

The luminescence of europium complex **72** [97] is switched off upon recognition of the copper(II) ion by the phenanthroline ligand. This is through electron transfer quenching of the phenanthroline singlet excited state by copper(II). As a result, the energy transfer sensitization efficiency to the europium ion is reduced. The addition of ethylenediamine tetraacetate to this fully quenched solution switches the emission back on. The switching effect is also observed with other transition metal ions such as iron(III), iron(II), and cobalt(II). However, the complex is about one to two orders of magnitude more sensitive to copper(II).

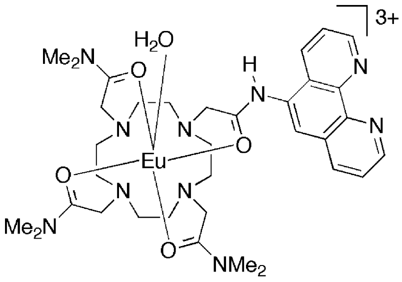

72

In the chemosensing ensemble approach, an analyte displaces a colorimetric or fluorescent indicator, which then changes its electronic or fluorescence spectrum. Coumarin 343 is hosted by dicopper complex **73** (Fig. 21) [98]. In this complex, the coumarin fluorescence is quenched due to an intracomplex electronic energy transfer process involving the copper ions. The coumarin is displaced by an analyte that binds to **73** with higher affinity, such as carbonate, giving rise to a complete recovery of the pristine coumarin fluorescence.

5. Metal complex-based molecular field-effect transistors

The switching phenomena described in the previous sections occur within individual molecules or supramolecules. Barring a few exceptions, however, the detection of the output signal, say, fluorescence, is done for a large ensemble of molecules. Recent developments in nanofabrication and STM techniques allow organic molecules and metal complexes to be subjected to electrical measurements at the single-molecule level. These studies are along the line toward potential applications in molecular electronics, in which individual molecules function as active

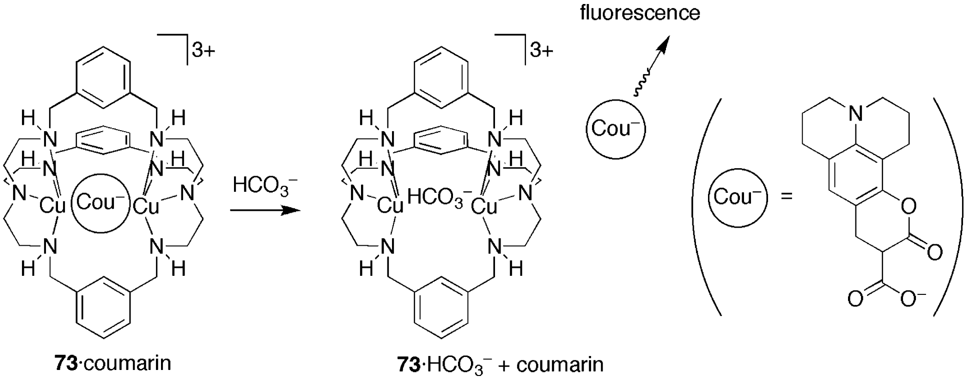

Fig. 21. Chemosensing ensemble [98].

components. The field-effect transistor (FET) is arguably the central component in modern electronics. It would be interesting to see whether or not individual molecules could replace semiconductors as an active channel in FETs. In this connection, transition metal complexes have been used in FET configurations, a schematic of which is illustrated in Fig. 22. A single molecule of a metal complex is immobilized in a narrow gap of less than a few nanometers between two metallic electrodes, which are placed on a gate electrode across a dielectric layer.

Cobalt-tpy complexes, **74** and **75** [99], divanadium complex **76** [100], and metal complexes of dipyridylpyrrole ligand **77** [101,102] have been studied for single-molecule properties. The current–voltage characteristics under controlled gate potentials were examined at low temperatures. Various quantum effects owing to the molecule were observed. A simplified model of the conductance through a single molecule in an FET configuration is illustrated in Fig. 23a. There are threshold bias voltages for the differential conductance to take non-zero values. This is because there is no molecular state in energy close to the Fermi level of the electrodes (Fig. 23a, middle). Gate voltage can modulate the energy levels of molecular orbitals. The differential conductance increases at certain gate voltages, at which one of the molecular orbitals matches the Fermi level of the electrodes (Fig. 23a, left and right). Under such circumstances, the redox state of the molecule is in equilibrium with a one-electron oxidized or reduced state. In the case of cobalt complexes **74** and **75**, this corresponds to the equilibrium between cobalt(II) and cobalt(III) species.

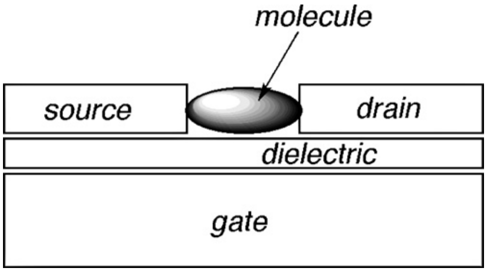

Fig. 22. Single-molecule FET.

There is another type of conduction near zero bias voltage at low temperatures by the coupling between an isolated spin and conduction electrons in the electrodes, which is called the Kondo effect. The presence of a spin in the molecule is the key to this phenomenon. The Kondo effect was observed for **75** with cobalt(II) ($S = 1/2$), monocationic **76**$^+$ ($S = 1/2$), and **77** with cobalt(II) ($S = 3/2$). Different redox states of these complexes, i.e., the cobalt(III) species and **76**°, which can be produced by varying the gate voltage, did not show the Kondo effect, highlighting the importance of the spin state in regard to this effect.

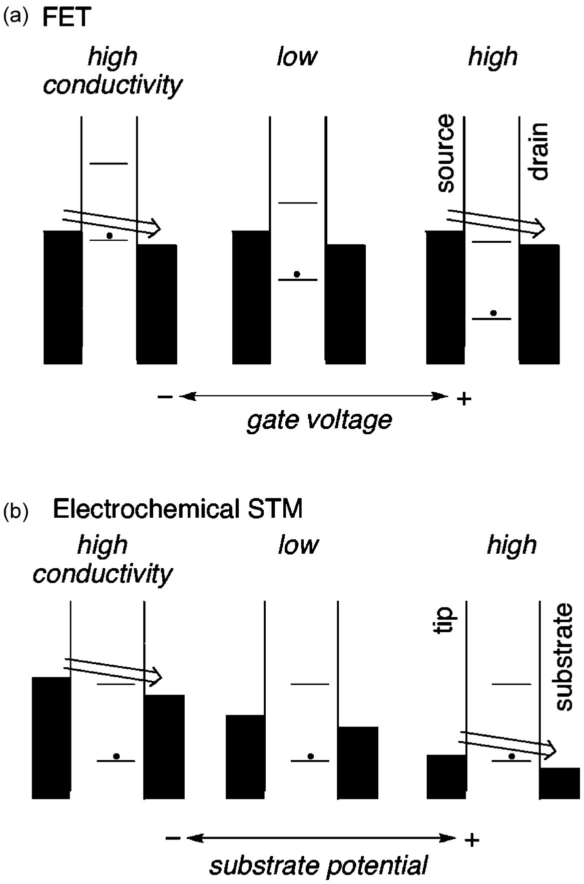

Fig. 23. Molecular field-effect transistors.

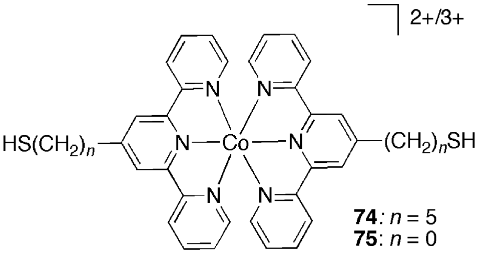

74: $n = 5$
75: $n = 0$

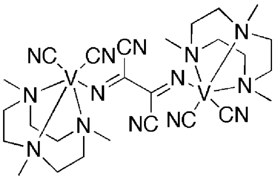

76

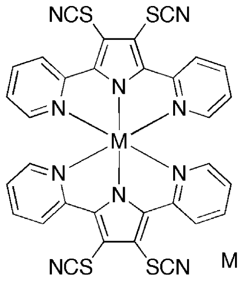

M = Co, Cu, Zn

77

Similar control over the redox state of molecules can be done with electrochemical STM (Fig. 23b). Here, the substrate potential can be controlled with respect to a reference electrode independently from the tip–substrate bias voltage. The differential conductance has a maximum when the substrate potential is close to one of the redox potentials of the molecule. Osmium complexes **79** and **80** immobilized on the surfaces of gold(1 1 1) and platinum(1 1 1), respectively, exhibit transistor-like behavior [103,104].

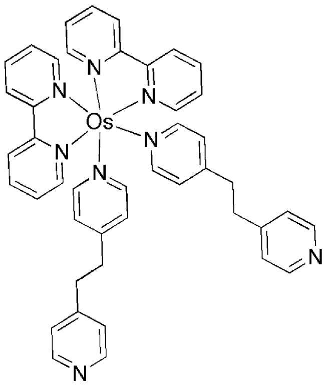

79

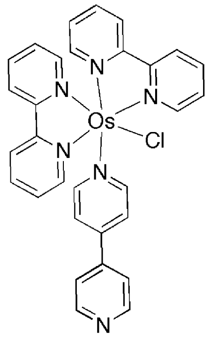

80

6. Conclusions and prospects

In this review article, we have described various metal complexes, in which electron and energy transfer processes are switched by externally applied signals. Electrons (redox reactions), light, and chemical species including protons, ions, and molecules, are used as the external stimuli. In the final section, electrical current switches in the form of FETs, which have a single-metal complex as the key component, are described.

In terms of practical utility, probably the chemical substance-controlled switches that produce optical signals, i.e. luminescence or absorbance changes, are the closest to applications in the field of molecular sensors. Beyond sensors, it is in principle possible for other types of switches responding to electrical and optical control signals to find use in molecular photonics and electronics devices. It is now possible to address the properties of individual molecules. It is envisaged that various types of metal complex-based switches, which have been proven to function in solution as described in this article, will be realized at the single-molecule level, not necessarily within the FET configurations. The next big challenges toward the realization of molecular electronics include how to integrate molecular components into functional assemblies. It is anticipated that the challenges will be overcome in coming years via self-assembly in combination with nanofabrication techniques. How to connect molecular systems with the outside macroscopic world is another big problem that should be addressed.

In this connection, the fabrication of ordered and programmed arrays of metal complexes is an important field of research. Recent years have seen a number of nanoscale molecular architectures on surfaces, some of which comprise metal complexes. Here, we will show only one example from our recent work just to provide a glimpse of what molecular nanoarchitecture can be, since these are beyond the scope of the present article. Iridium complexes $\mathbf{81}_n$ equipped with long alkyl chains, form ordered arrays on the surface of highly oriented pyrolytic graphite, as shown by the STM image and the schematics in Fig. 24 [105]. It was implied by cyclic voltammetry that there is significant intermolecular, let alone molecule–substrate, electronic interactions likely along the molecular rows in the assembly. Incorporation of functions (e.g., switchability) in such an ordered array will be one of the important research targets.

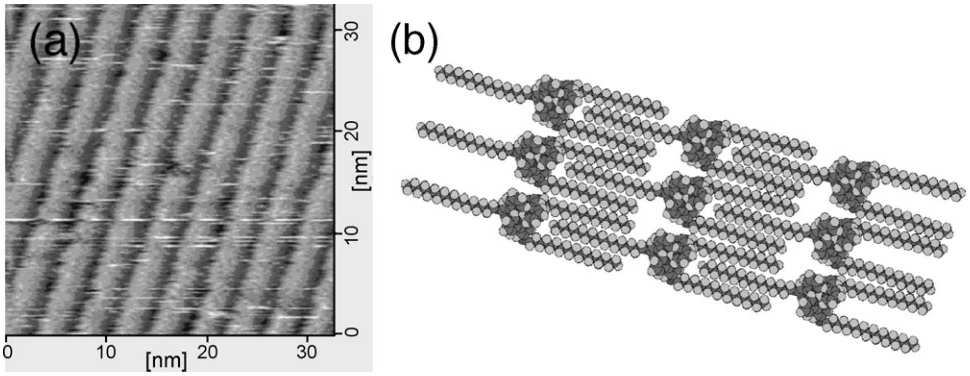

Fig. 24. The array of $\mathbf{81_{18}}$ on the surface of highly oriented pyrolytic graphite. (a) STM image. (b) Molecular arrangement in the array. Adapted from Ref. [105].

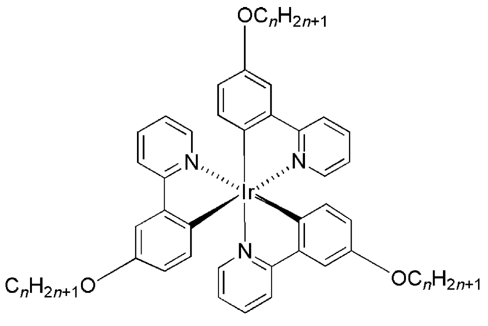

$\mathbf{81}_n$

It is likely that metal complexes play key roles in prospective molecular photonics and electronics devices, given the fact that, firstly, the electronic and optical properties of metal complexes can be changed in a controlled fashion and, secondly, the metal complexes are excellent building blocks for organized molecular architectures owing to their well-defined coordination interactions.

Acknowledgements

Our work described in this article was partially supported by the Ministry of Education, Culture, Sports, Science and Technology, Japan, through the programs of the Grant-in-Aid for Scientific Research and the High Tech Research Center Project for Private Universities.

References

[1] B.L. Feringa (Ed.), Molecular Switches, Wiley-VCH, Weinheim, 2001.
[2] V. Balzani, A. Credi, M. Venturi, Molecular Devices and Machines—A Journey into the Nano World, Wiley-VCH, Weinheim, 2003.
[3] L. De Cola, P. Belser, Coord. Chem. Rev. 177 (1998) 301.
[4] F. Barigelletti, L. Flamigni, Chem. Soc. Rev. 29 (2000) 1.
[5] A.C. Benniston, Chem. Soc. Rev. 33 (2004) 573.
[6] P.J. Low, Dalton (2005) 2821.
[7] V. Goulle, A. Harriman, J.-M. Lehn, J. Chem. Soc. Chem. Commun. (1993) 1034.
[8] S. Arounaguiri, B.G. Maiya, Inorg. Chem. 38 (1999) 842.
[9] A.C. Benniston, G.M. Chapman, A. Harriman, S.A. Rostron, Inorg. Chem. 44 (2005) 4029.
[10] R. Martínez, I. Ratera, A. Tárraga, P. Molina, J. Veciana, Chem. Commun. (2006) 3809.
[11] R. Bergonzi, L. Fabbrizzi, M. Licchelli, C. Mangano, Coord. Chem. Rev. 170 (1998) 31.
[12] V. Amendola, L. Fabbrizzi, F. Foti, M. Licchelli, C. Mangano, P. Pallavicini, A. Poggi, D. Sacchi, A. Taglietti, Coord. Chem. Rev. 250 (2006) 273.
[13] G. De Santis, L. Fabbrizzi, M. Licchelli, C. Mangano, D. Sacchi, Inorg. Chem. 34 (1995) 3581.
[14] G. De Santis, L. Fabbrizzi, M. Licchelli, N. Sardone, A.H. Velders, Chem. Eur. J. 2 (1996) 1243.
[15] M.D. Casa, L. Fabbrizzi, M. Licchelli, A. Poggi, D. Sacchi, M. Zema, J. Chem. Soc. Dalton Trans. (2001) 1671.
[16] L. Fabbrizzi, M. Licchelli, S. Mascheroni, A. Poggi, D. Sacchi, M. Zema, Inorg. Chem. 41 (2002) 6129.
[17] J. Otsuki, K. Sato, M. Tsujino, N. Okuda, K. Araki, M. Seno, Chem. Lett. (1996) 847.
[18] J. Otsuki, D.-M. Li, K. Sato, A. Nakagome, T. Takido, I. Yoshikawa, T. Akasaka, K. Araki, Bull. Chem. Soc. Jpn. 76 (2003) 1185.
[19] T. Hirao, K. Iida, Chem. Commun. (2001) 431.
[20] R. Lomoth, T. Häupl, O. Johansson, L. Hammarström, Chem. Eur. J. 8 (2002) 102.
[21] E. Zahavy, M.A. Fox, Chem. Eur. J. 4 (1998) 1647.
[22] J. Otsuki, Trends Phys. Chem. 8 (2001) 61.
[23] J. Otsuki, K. Harada, K. Araki, Chem. Lett. (1999) 269.
[24] X. Xiao, W. Xu, D. Zhang, H. Xu, H. Lu, D. Zhu, J. Mater. Chem. 15 (2005) 2557.
[25] G. Will, G. Boschloo, R. Hoyle, S.N. Rao, D. Fitzmaurice, J. Phys. Chem. B 102 (1998) 10272.
[26] G.D. Will, G. Boschloo, S.N. Rao, D. Fitzmaurice, J. Phys. Chem. B 103 (1999) 8067.
[27] A. Merrins, C. Kleverlaan, G. Will, S.N. Rao, F. Scandola, D. Fitzmaurice, J. Phys. Chem. B 105 (2001) 2998.
[28] G. Will, J. Sotomayor, S.N. Rao, D. Fitzmaurice, J. Mater. Chem. 9 (1999) 2297.
[29] R. Clérac, F.A. Cotton, K.R. Dunbar, C.A. Murillo, I. Pascual, X. Wang, Inorg. Chem. 38 (1999) 2655.
[30] J.F. Berry, F.A. Cotton, L.M. Daniels, C.A. Murillo, J. Am. Chem. Soc. 124 (2002) 3212.
[31] C.-Y. Yeh, Y.-L. Chiang, G.-H. Lee, S.-M. Peng, Inorg. Chem. 41 (2002) 4096.
[32] J.F. Berry, F.A. Cotton, P. Lei, T. Lu, C.A. Murillo, Inorg. Chem. 42 (2003) 3534.
[33] I.-W.P. Chen, M.-D. Fu, W.-H. Tseng, J.-Y. Yu, S.-H. Wu, C.-J. Ku, C. Chen, S.-M. Peng, Angew. Chem. Int. Ed. 45 (2006) 5814.
[34] R.W. Wagner, J.S. Lindsey, J. Seth, V. Palaniappan, D.F. Bocian, J. Am. Chem. Soc. 118 (1996) 3996.
[35] R.K. Lammi, R.W. Wagner, A. Ambroise, J.R. Diers, D.F. Bocian, D. Holten, J.S. Lindsey, J. Phys. Chem. B 105 (2001) 5341.
[36] D. Holten, D.F. Bocian, J.S. Lindsey, Acc. Chem. Res. 35 (2002) 57.
[37] J. Otsuki, M. Tsujino, T. Iizaki, K. Araki, M. Seno, K. Takatera, T. Watanabe, J. Am. Chem. Soc. 119 (1997) 7895.
[38] C. Kaes, A. Katz, M.W. Hosseini, Chem. Rev. 100 (2000) 3553.

[39] H. Hofmeier, U.S. Schubert, Chem. Soc. Rev. 33 (2004) 373.
[40] T. Akasaka, J. Otsuki, K. Araki, Chem. Eur. J. 8 (2002) 130.
[41] T. Akasaka, T. Mutai, J. Otsuki, K. Araki, Dalton Trans. (2003) 1537.
[42] V. Amendola, L. Fabbrizzi, P. Pallavicini, E. Sartirana, A. Taglietti, Inorg. Chem. 42 (2003) 1632.
[43] C.A. Hunter, L.D. Sarson, Tetrahedron Lett. 37 (1996) 699.
[44] A.J. Myles, N.R. Branda, Tetrahedron Lett. 41 (2000) 3785.
[45] L. Fabbrizzi, M. Licchelli, L. Parodi, A. Poggi, A. Taglietti, J. Fluoresc. 8 (1998) 263.
[46] J. Otsuki, A. Suka, K. Yamazaki, H. Abe, Y. Araki, O. Ito, Chem. Commun. (2004) 1290.
[47] J. Otsuki, K. Narutaki, J.M. Bakke, Chem. Lett. 33 (2004) 356.
[48] J. Otsuki, K. Narutaki, Bull. Chem. Soc. Jpn. 77 (2004) 1537.
[49] M. Andersson, L.E. Sinks, R.T. Hayes, Y. Zhao, M.R. Wasielewski, Angew. Chem. Int. Ed. 42 (2003) 3139.
[50] M.P. Debreczeny, W.A. Svec, M.R. Wasielewski, Science 274 (1996) 584.
[51] D. Gosztola, M.P. Niemczyk, M.R. Wasielewski, J. Am. Chem. Soc. 120 (1998) 5118.
[52] R.T. Hayes, M.R. Wasielewski, D. Gosztola, J. Am. Chem. Soc. 122 (2000) 5563.
[53] S. Fraysse, C. Coudret, J.-P. Launay, Eur. J. Inorg. Chem. (2000) 1581.
[54] V. Adamo, P. Belser, Chimia 57 (2003) 169.
[55] R.T.F. Jukes, V. Adamo, F. Hartl, P. Belser, L. De Cola, Inorg. Chem. 43 (2004) 2779.
[56] P. Belser, L. De Cola, F. Hartl, V. Adamo, B. Bozic, Y. Chriqui, V.M. Iyer, R.T.F. Jukes, J. Kühni, M. Querol, S. Roma, N. Salluce, Adv. Funct. Mater. 16 (2006) 195.
[57] R. Sakamoto, M. Murata, H. Nishihara, Angew. Chem. Int. Ed. 45 (2006) 4793.
[58] A. Amini, K. Bates, A.C. Benniston, D.J. Lawrie, E. Soubeyrand-Lenoir, Tetrahedron Lett. 44 (2003) 8245.
[59] D.S. Tyson, C.A. Bignozzi, F.N. Castellano, J. Am. Chem. Soc. 124 (2002) 4562.
[60] A.P. de Silva, H.Q.N. Funaratne, T. Gunnlaugsson, A.J.M. Huxley, C.P. McCoy, J.T. Fademacher, T.E. Rice, Chem. Rev. 97 (1997) 1515.
[61] A.P. de Silva, N.D. McClenaghan, Chem. Eur. J. 10 (2004) 574.
[62] D. Parker, Coord. Chem. Rev. 205 (2000) 109.
[63] T. Gunnlaugsson, J.P. Leonard, Chem. Commun. (2005) 3114.
[64] A.P. de Silva, H.Q.N. Gunaratne, T.E. Rice, Angew. Chem. Int. Ed. Engl. 35 (1996) 2116.
[65] A.P. de Silva, H.Q.N. Gunaratne, T.E. Rice, S. Stewart, Chem. Commun. (1997) 1891.
[66] L. Fabbrizzi, M. Licchelli, C. Rospo, D. Sacchi, M. Zema, Inorg. Chim. Acta 300-302 (2000) 453.
[67] M.D. Ward, Chem. Soc. Rev. (1995) 121.
[68] S.F. Nelsen, Chem. Eur. J. 6 (2000) 581.
[69] K.D. Demadis, C.M. Hartshorn, T.J. Meyer, Chem. Rev. 101 (2001) 2655.
[70] J.-P. Launay, Chem. Soc. Rev. 30 (2001) 386.
[71] J.-P. Launey, M. Tourrel-Pagis, J.-F. Lipskier, V. Marvaud, C. Joachim, Inorg. Chem. 30 (1991) 1033.
[72] M. Haga, T. Ano, K. Kano, S. Yamabe, Inorg. Chem. 30 (1991) 3843.
[73] M. Haga, M.M. Ali, S. Koseki, K. Fujimoto, A. Yoshimura, K. Nozaki, T. Ohno, K. Nakajima, D.J. Stufkens, Inorg. Chem. 35 (1996) 3335.
[74] R.C. Rocha, H.E. Toma, Inorg. Chem. Commun. 4 (2001) 230.
[75] P.D. Beer, V. Timoshenko, M. Maestri, P. Passaniti, V. Balzani, Chem. Commun. (1999) 1755.
[76] P.D. Beer, E.J. Hayes, Coord. Chem. Rev. 240 (2003) 167.
[77] I. Bruseghini, L. Fabbrizzi, M. Licchelli, A. Taglietti, Chem. Commun. (2002) 1348.
[78] V. Amendola, L. Fabbrizzi, C. Mangano, P. Pallavicini, A. Perotti, A. Taglietti, J. Chem. Soc. Dalton Trans. (2000) 185.
[79] V. Amendola, L. Fabbrizzi, C. Mangano, H. Miller, P. Pallavicini, A. Perotti, A. Taglietti, Angew. Chem. Int. Ed. 41 (2002) 2553.
[80] R. Ballardini, V. Balzani, M. Clemente-León, A. Credi, M.T. Gandolfi, E. Ishow, J. Perkins, J.F. Stoddart, H.-R. Tseng, S. Wenger, J. Am. Chem. Soc. 124 (2002) 12786.
[81] B. Ferrer, G. Rogez, A. Credi, R. Ballardini, M.T. Gandolfi, V. Balzani, Y. Liu, H.-R. Tseng, J.F. Stoddart, Proc. Natl. Acad. Sci. U.S.A. 103 (2006) 18411.
[82] A.S.D. Sandanayaka, Y. Araki, O. Ito, R. Chitta, S. Gaddeb, F. D'Souza, Chem. Commun. (2006) 4327.
[83] C.-S. Choi, T. Mutai, S. Arita, K. Araki, J. Chem. Soc. Perkin Trans. (2000) 243.
[84] C.-S. Choi, L. Mishra, T. Mutai, K. Araki, Bull. Chem. Soc. Jpn. 73 (2000) 2051.
[85] T. Akasaka, H. Inoue, M. Kuwabara, T. Mutai, J. Otsuki, K. Araki, Dalton Trans. (2003) 815.
[86] M.P. Lowe, D. Parker, Inorg. Chem. Acta 317 (2001) 163.
[87] D. Parker, J.A.G. Williams, Chem. Commun. (1998) 245.
[88] D. Parker, P.K. Senanayake, J.A.G. Williams, J. Chem. Soc., Perkin Trans. 2 (1998) 2129.
[89] L. Fabbrizzi, M. Licchelli, P. Pallavicini, L. Parodi, Angew. Chem. Int. Ed. Engl. 37 (1998) 800.
[90] L. Fabbrizzi, F. Foti, M. Licchelli, P.M. Maccarini, D. Sacchi, M. Zema, Chem. Eur. J. 8 (2002) 4965.
[91] R.W. Wagner, T.E. Johnson, J.S. Lindsey, J. Am. Chem. Soc. 118 (1996) 11166.
[92] J.-S. Hsiao, B.P. Krueger, R.W. Wagner, T.E. Hohnson, J.K. Delaney, D.C. Mauzerall, G.R. Gleming, J.S. Linsey, D.G. Bocian, R.J. Donohoe, J. Am. Chem. Soc. 118 (1996) 11181.
[93] J. Seth, V. Palaniappan, R.W. Wagner, T.E. Johnson, J.S. Lindsey, D.F. Bocian, J. Am. Chem. Soc. 118 (1996) 11194.
[94] J. Otsuki, A. Yasuda, T. Takido, Chem. Commun. (2003) 608.
[95] J. Otsuki, Y. Kato, T. Sasahara, K. Iwasaki, A. Yasuda, Chem. Lett. 34 (2005) 1684.
[96] J. Otsuki, K. Iwasaki, Y. Nakano, M. Itou, Y. Araki, O. Ito, Chem. Eur. J. 10 (2004) 3461.
[97] T. Gunnlaugsson, J.P. Leonard, K. Sénéchal, A.J. Harte, Chem. Commun. (2004) 782.
[98] L. Fabbrizzi, A. Leone, A. Taglietti, Angew. Chem. Int. Ed. Engl. 40 (2001) 3066.
[99] J. Park, A.N. Pasupathy, J.I. Goldsmith, C. Chang, Y. Yaish, J.R. Petta, M. Rinkoski, J.P. Sethna, H.D. Abruña, P.L. McEuen, D.C. Ralph, Nature 417 (2002) 722.
[100] W. Liang, M.P. Shores, M. Bockrath, J.R. Long, H. Park, Nature 417 (2002) 725.
[101] L.H. Yu, Z.K. Keane, J.W. Ciszek, L. Cheng, J.M. Tour, T. Baruah, M.R. Pederson, D. Natelson, Phys. Rev. Lett. 95 (2005) 256803.
[102] D. Natelson, L.H. Yu, J.W. Ciszek, Z.K. Keane, J.M. Tour, Chem. Phys. 324 (2006) 267.
[103] T. Albrecht, A. Guckian, J. Ulstrup, J.G. Vos, Nano Lett. 5 (2005) 1451.
[104] T. Albrecht, A. Guckian, A.M. Kuznetsov, J.G. Vos, J. Ulstrup, J. Am. Chem. Soc. 128 (2006) 17132.
[105] J. Otsuki, T. Tokimoto, Y. Noda, T. Yano, T. Hasegawa, X. Chen, Y. Okamoto, Chem. Eur. J. 13 (2007) 2311.